The Role of Population Games and Evolutionary Dynamics in Distributed Control Systems

Nicanor Quijano, Carlos Ocampo-Martinez, Julian Barreiro-Gomez,
German Obando, Andres Pantoja, Eduardo Mojica-Nava
POC: C. Ocampo-Martinez (cocampo@iri.upc.edu)

Recently, there has been an increasing interest in studying large-scale distributed systems in the control community. Efforts have been invested in developing several techniques wishing to address the main challenges found in this kind of problems, for instance, the amount of information to guarantee the proper operation of the system and the economic costs associated to the required communication structure. Moreover, another issue appears when there is a large amount of required data to control the system. The measuring and transmission processes, and the computation of the control inputs make closed-loop systems suffer from high computational burden.

One way to overcome such problems is to consider the use of multi-agent systems framework, which may be cast in game-theoretical terms. Game theory studies interactions between self-interested agents. Particularly, this theory tackles with the problem of interaction between agents using different strategies that wish to maximize their welfares. For instance in [1], the authors provide connections between games, optimization, and learning for signal processing in networks. Other approaches in terms of learning and games can be found in [2]. In [3], distributed computation algorithms are developed based on generalized convex games that do not require full information, and where there is a dynamic change in terms of network topologies. Applications of game theory in control of optical networks and game-theoretic methods for smart grids are described in [4], [5], [6]. Another approach in game theoretical methods is to design protocols or mechanisms that possess some desirable properties [7]. This approach leads to a broad analysis of multi-agent interactions, particularly those involving negotiation and coordination problems [8]. Other game-theoretical applications to engineering are reported in [9].

From a game-theoretical perspective, it can be distinguished among three types of games: matrix games, continuous games, and differential/dynamic games (see "The relationship among matricial games, full-potential population games, and resource allocation problems"). In matrix games (that generally use the normal form), individuals play simultaneously and only once, and the decision is mainly based on a static terms. In this case, players or agents are individually treated. Differently, in continuous games, players have infinitely many pure strategies [10], [11]. On the other hand, in dynamic games it is assumed that players can use some type of learning mechanism that allows them to adjust the actions taken based on their past decisions. Basically, it can be said that dynamic games are characterized by three main problems: i) how to model the environment where players interact; ii) how to model the objectives of players; and iii) how to specify the order in which the actions are taken and how much information each player possesses. In this case, it is assumed that there are interactions between large number of agents (which are usually unknown) [12].

Among these dynamic games, there exist the evolutionary game dynamics, which are

dynamic processes that describe how the aggregate behavior of the agents changes over time [13]. Evolutionary game theory (EGT) was first studied by Fisher, while he was trying to explain the approximate equality of the sex ratio in mammals [14]. However, it is said that the area bloomed with the appearance of the seminal article *The Logic of Animal Conflict* by Maynard Smith and Price in 1973, where the concept of evolutionarily stable strategy (ESS) was originally defined [15]. Since then, several works have been published mainly in biology [16], [17] due to the usefulness of the ESS concept to explain several behaviors that emerge in nature. However, there exists another approach to understand EGT. This approach is based on the dynamic foundations of the ESS concept, which were firstly introduced by Taylor and Jonker in 1978 providing the replicator dynamics [18]. Later on, it was proved that the replicator nonlinear differential equation can also be addressed from an economic perspective, using models in imitation among populations of economic agents [13]. The combination of *population games* (which describe strategic interactions among large number of small and anonymous agents) and a *revision protocol* (which specifies how agents can choose and change strategies) leads to a dynamic process describing the behavior of agents in time called *evolutionary game dynamics* [13]. Modeling strategic interactions of agents in large-scale systems is more suitable from this perspective, since the evolution of the agents behavior is better described by the differential equation that captures this process [19].

Some applications of EGT in engineering problems can be found along different fields. For instance, wind farms control [20], [21], multiple access control for communication systems [22], cyber security [23], combinatorial optimization [24], bandwidth allocation [25], hierarchical frequency control in microgrids [26], dispatch of electric generators [27], building temperature control [28], constrained extremum seeking [29], and control of drinking water networks [30], among others.

There are three main advantages of using EGT in engineering problems. The first motivation is that the analogy between games and engineering problems is straightforward in a large variety of cases. For instance, a control problem can be viewed as a game where the available control inputs are associated to strategies, and the control objective is expressed in terms of payoff functions. There are several examples of the aforementioned analogy in the literature. For example, in [21], authors report the design of a power-wind farm control by taking as strategies the axial induction factors of the wind turbines; in [31] and [32], authors develop a controller to optimally distribute flows between different reservoirs in water systems, which are taken as strategies into the underlying game.

The second motivation to use an EGT approach is the relationship between the solution of a game given by a Nash equilibrium and the solution of optimization problems. In this regard, it has been proven that, under certain conditions, the Nash equilibrium satisfies the Karush-Kuhn-Tucker (KKT) first-order conditions of constrained optimization problems [13]. This property has been exploited in many works such as [30], where distributed optimization problems are addressed by using potential games and population dynamics. In [33], a general analysis of state-based potential games is presented and the growing interest in the application of game-theoretic methods to the design and control of multi-agent systems is discussed.

Finally, the third motivation for using an EGT approach is that the solution of games can be obtained by employing local information [34], [35]. In [20], local rules are designed in order to achieve a global objective. Additionally, in [36] the issue of dealing with coupled constraints is solved by decoupling such constraints using local rules. Therefore, if a game framework is applied to address an engineering problem, distributed methodologies emerge. This

feature is quite relevant since nowadays the complexity of systems is increasing permanently, which makes the implementation of centralized approaches expensive or even infeasible. In this regard, the appealing features of distributed population dynamics can be exploited in several applications. For instance, it has been shown that distributed population dynamics can be used in the design of constrained optimization algorithms and in the synthesis of control systems for problems requiring non-centralized schemes. Compared to other distributed techniques such as dual decomposition methods [37], the implementation of distributed population dynamics does not need the inclusion of a centralized coordinator. This key property reduces the cost of the required communication infrastructure. Furthermore, some families of distributed population dynamics (for instance, distributed replicator dynamics and distributed Smith dynamics) naturally address nonnegativity constraints that emerge in a variety of problems due to physical limitations (for instance, in scheduling problems, the time allocated to each task cannot be negative). Although nonnegativity constraints are tackled in other distributed approaches by means of barrier functions, it is known that the use of those functions carries out some problems related to the convergence rate and the accuracy of the solution, especially for large-scale problems [38].

An outstanding advantage of distributed population dynamics compared to distributed learning algorithms for normal-form games is that classic learning techniques fail in applications that include constraints involving all the decision variables (this drawback has been pointed out in [33]). Under this scenario, distributed population dynamics become a proper alternative since their trajectories evolve towards the optimal solution satisfying a coupled constraint associated to the mass of the population that is involved in the strategic game. This property can be exploited for solving dynamic resource allocation problems.

One crucial engineering problem where dynamic resource allocation is paramount consists in the design of a smart city (SC) [39]. An SC can be seen as an organic system that is in charge of connecting and controlling different subsystems and components in order to have a *perfect* behavior. In other words, the SC is like an intelligent control similar to the human being, which must handle different services through a communication backbone [40]. Among the emerging problems associated to such systems are those related with water and energy. In this article, three emergent problems in SC are addressed: smart lighting, optimal economic dispatch in microgrids, and control of urban drainage systems (UDS).

Lighting systems represent a high energy consumption in buildings, such that reaching comfortable illuminance levels require distributed control strategies to deal with energy saving, daylight harvesting, and cross-illumination effects. Then, with the adaptation of a population-based methodology, limited power resources are split among lamps of several zones taking into account local controllers exchanging information within a communication network and different lighting environments.

On the other hand, the frequency control in microgrids is one of the fundamental problem in the context of smart grids. In particular, the dynamical optimal dispatch of active power of distributed generators is solved as a dynamic resource allocation problem using population games. Conventional dispatch problem in power systems consists in either minimizing the total generation cost or maximizing the total utility of all generators, while restrictions over both power balance and generation capacity are satisfied [41]. Traditionally, the economic dispatch problem has been solved by using static optimization algorithms [42], or direct search methods [43], which operate off-line in a time interval between 5 minutes to 1 hour [37]. This traditional dispatch algorithm requires a centralized controller with a high-bandwidth communication infrastructure

as the number of nodes increase to handle information from each node within the distribution system. Therefore, distributed control algorithms such as the distributed population games are becoming promising approaches in the context of smart grids since they can be more robust and resilient to network variations. To analyze the effects of the communication infrastructure in the optimal dispatch algorithm, it has been proposed a distributed version of the replicator dynamics algorithm to respond dynamically to the needs of the microgrid assuming that no full information is available.

Finally, the real-time control design of UDS is challenging since these large-scale systems involve a large number of states and control inputs. Besides, they are affected by exogenous disturbances given by rain events. As a convenient and suitable solution, it is shown that the control of UDS can be addressed as a resource allocation problem, and that the entire UDS may be divided into several sub-systems locally controlled by using population-dynamics-based strategies.

Population Games

Preliminary Concepts

Population games describe the strategic interaction of large populations of players. Different from normal-form games, where players are individually treated, in population games players are grouped in a continuum of mass denoted by $m \in \mathbb{R}_{>0}$. Thus, in this framework, each individual of the population corresponds to a quantum of that mass. Besides, individuals can choose their actions to play from a set of pure available strategies denoted by $\mathcal{S}$. This set of strategies is finite and, for convention, strategies are indexed using natural numbers. Hence, for a game with n available strategies, the set of strategies is given by $\mathcal{S} = \{1, ..., n\}$. For instance, in the classic network-routing game, each element of the set $\mathcal{S}$ is associated with an available route of the network. An assumption of population games is that all players have the same set of strategies. However, it is worth noting that multiple set of strategies can be introduced in the formulation of population games by using a framework known as multi-population (this topic is out of the scope of this article).

Since in population games the number of players is large, strategy profiles are not described by the actions of all players as is usual in normal-form games. In fact, strategy profiles of population games are characterized by the distribution of the mass of players m among the available strategies. For instance, in a game with two available strategies where exactly one half of the population chooses the first strategy and the other half chooses the second strategy, the strategy profile is given by $(\frac{m}{2}, \frac{m}{2})$. Strategy profiles of population games are called *population states*. To formalize the notation of population states, the nonnegative scalars $p_1, \ldots, p_n$ are defined, where p_i denotes the portion of the mass of players that chooses the strategy $i \in \mathcal{S}$. Thus, the vector $\mathbf{p} = [p_1, \ldots, p_n]^\top$ denotes the population state. The set of possible population states, which corresponds to all possible distributions of individuals among the strategies, is given by the following simplex

$$\Delta = \left\{ \mathbf{p} \in \mathbb{R}^n_{\geq 0} : \sum_{i \in \mathcal{S}} p_i = m \right\}. \tag{1}$$

Individuals that choose the ith strategy to play obtain a reward that depends on the

population state. This reward is captured by a payoff function $f_i : \Delta \to \mathbb{R}$ (within the biology framework, the payoff function is usually called *fitness function*). Hence, for a given population state $\mathbf{p}$, $f_i(\mathbf{p})$ specifies the reward associated with the strategy $i \in \mathcal{S}$. A population game is completely characterized by the payoff vector $\mathbf{f} : \Delta \mapsto \mathbb{R}^n$, where $\mathbf{f}(\mathbf{p}) = [f_1(\mathbf{p}), \dots, f_n(\mathbf{p})]^\top$.

As in normal-form games, Nash equilibrium is the most commonly used solution concept in population games since in a Nash equilibrium each individual of the population is playing the best possible strategy against a given population state. Formally, the concept of Nash equilibria of population games is introduced in Definition 1.

Definition 1: **Nash Equilibria** (adapted from [13]). A population state $\mathbf{p}^* \in \Delta$ is a Nash equilibrium if each used strategy entails the maximum benefit for those players who choose it. Equivalently, the set of Nash equilibria is given by $NE = \{\mathbf{p}^* \in \Delta : p_i^* > 0 \Rightarrow f_i(\mathbf{p}^*) \geq f_j(\mathbf{p}^*), \text{ for all } i, j = 1, \dots, n\}$.

$\diamondsuit$

According to Definition 1, if the population adopts a Nash equilibrium, individuals cannot improve their benefit by changing their strategy. Therefore, under the assumption that the individuals are rational (that is, they try to maximize their payoff), Nash equilibria are natural candidates to be the output of a population game. In fact, a key result in game theory states that every population game has at least one Nash equilibrium [13]. However, this fact does not imply that populations involved in strategic interactions necessarily adopt Nash equilibria. Forthcoming sections explore the conditions for guaranteeing convergence of the population state to a Nash equilibrium.

Strategy-constrained interactions

Players of the population encounter each other and interact according to the framework described above. Traditionally, these encounters do not depend on the strategies played by the individuals. In other words, encounters between individuals playing the ith strategy and individuals playing j^{th} strategy are allowed no matter what i and j are (e.g., see Figure S1(a)). Nonetheless, in the more general framework proposed in [44], interactions among players are strategy-constrained.

Following the approach reported in [44], the strategy-constrained interactions can be modeled by using an undirected graph $\mathcal{G} = \{\mathcal{V}, \mathcal{E}\}$. The set of nodes $\mathcal{V}$ is associated with the available strategies, that is, $\mathcal{V} = \mathcal{S}$, and the set of edges $\mathcal{E} \subset \mathcal{V} \times \mathcal{V}$ describes the allowed interactions between individuals playing different strategies. Hence, if $(i, j) \in \mathcal{E}$, then an individual playing strategy i can be matched with an individual playing strategy j. On the other hand, if $(i, j) \notin \mathcal{E}$, then individuals playing strategies i and j cannot encounter each other (for further details, the reader is referred to [44]).

Figure 1 shows the graph representation of two different interaction scenarios for the same population. Notice that populations where interactions are not strategy-constrained are represented by complete graphs since individuals playing any pair of strategies can encounter each other. By contrast, populations under strategy-constrained interactions are represented by non-complete graphs due to the fact that the encounter between individuals depends on the strategies that these individuals are playing. In [44], strategy-constrained interactions are employed to model local information structures.

Population Dynamics

Nash equilibrium predicts the outcome of a population game. Different from this static notion, there exists a framework capable to model not only the outcome of a population game, but also the evolution of the population state along the time. This framework is called *population dynamics*, and its fundamental input is the concept of *revision protocol*.

A revision protocol can be seen as a set of rules that allows the individuals to take decisions. Specifically, a revision protocol establishes conditions under which an individual changes its strategy. Formally, Definition 2 introduces the concept of revision protocol.

Definition 2: **Revision Protocol** (adapted from [13]). A revision protocol, denoted by $\rho = [\rho_{ij}]$, is a map $\rho : \mathbb{R}^n \times \Delta \mapsto \mathbb{R}^{n \times n}_{\geq 0}$ characterized by the conditional switch rates $\{\rho_{ij} : i, j \in \mathcal{S}\}$. Given a population state $\mathbf{p}$ and a payoff vector $\mathbf{f}(\mathbf{p})$, $\rho_{ij}(\mathbf{f}(\mathbf{p}), \mathbf{p})$ captures the switch rate from the ith strategy to the jth strategy. $\diamondsuit$

The dynamical process induced by revision protocols can be described as follows: at each time instant, an individual of the population is randomly selected and receives a revision opportunity. If an individual playing the ith strategy is selected, it switches to the jth strategy with probability proportional to $\rho_{ij}(\mathbf{f}(\mathbf{p}), \mathbf{p})$. Assuming that interactions among individuals of the population are not strategy-constrained, the process described above is modeled with the following dynamics

$$\dot{p}_i = \sum_{j \in \mathcal{S}} p_j \rho_{ji}(\mathbf{f}(\mathbf{p}), \mathbf{p}) - p_i \sum_{j \in \mathcal{S}} \rho_{ij}(\mathbf{f}(\mathbf{p}), \mathbf{p}), \text{ for all } i \in \mathcal{S}, \tag{2}$$

which correspond to the *mean dynamics* [13]. The first term of the right-hand-side of (2) models the inflow of players to the ith strategy (that is, individuals that switch from other strategies to the ith strategy), while the second term models the outflow of players from the ith strategy (that is, individuals that change strategy $i \in \mathcal{S}$ by another strategy).

Summarizing, (2) models the dynamics of a population involved in a strategic game that is using a given revision protocol. In this regard, different revision protocols produce different population dynamics models. The most studied dynamics in the literature are listed below.

- The pairwise proportional imitation protocol $\rho_{ij} = p_j[f_j(\mathbf{p}) - f_i(\mathbf{p})]_+$, where $[\cdot]_+ := \max(\cdot, 0)$, leads to the *replicator dynamics*, which are characterized by the following differential equation

$$\dot{p}_i = p_i \left(f_i(\mathbf{p}) - \bar{f} \right), \text{ for all } i \in \mathcal{S}, \tag{3}$$

  where $\bar{f} := \frac{1}{m} \sum_{j=1}^{n} p_j f_j(\mathbf{p})$ is known as the *average payoff function*. Replicator dynamics were introduced by Taylor and Jonker in 1978 [18]. These dynamics are largely studied in biology, being the first game dynamics used to describe evolutionary game theory. From a biological point of view, replicator dynamics capture the natural selection process where the size of the most successful populations (that is, those with a payoff higher than the average) increases while the size of the less successful ones decreases.

- The pairwise comparison protocol $\rho_{ij} = [f_j(\mathbf{p}) - f_i(\mathbf{p})]_+$ produces the *Smith dynamics*, which are given by

$$\dot{p}_i = \sum_{j=1}^{n} p_j \left[f_i(\mathbf{p}) - f_j(\mathbf{p}) \right]_+ - p_i \sum_{j=1}^{n} \left[f_j(\mathbf{p}) - f_i(\mathbf{p}) \right]_+, \text{ for all } i \in \mathcal{S}. \tag{4}$$

The Smith dynamics were proposed by Smith in 1984 [45]. Smith used these dynamics to describe traffic assignment, which is a class of congestion game that emerges in transportation problems. Different from replicator dynamics, Smith dynamics satisfy Nash stationarity. This latter concept means that the set of equilibrium points of the Smith dynamics is equal to the set of Nash equilibria of the underlying population game.

- The logit choice protocol $\rho_{ij} = \frac{e^{\eta^{-1} f_j(\mathbf{p})}}{\sum\limits_{k \in \mathcal{S}} e^{\eta^{-1} f_k(\mathbf{p})}}$, where $\eta > 0$ is known as noise level, generates the logit dynamics

$$\dot{p}_i = \frac{e^{\eta^{-1} f_i(\mathbf{p})}}{\sum\limits_{k \in \mathcal{S}} e^{\eta^{-1} f_k(\mathbf{p})}} - p_i, \text{ for all } i \in \mathcal{S}. \tag{5}$$

The logit dynamics, which are used to represent bounded rationality of players, were first introduced by Blume in 1993 [46]. If $\eta \to 0$, then players are completely rational, and they only choose the best possible strategies under the current population state. Nonetheless, if the noise level η increases, then players can choose strategies that are not best responses (indeed, if $\eta \to +\infty$, individuals play strategies nearly at random). This last situation models scenarios in which players have either a limited knowledge of the game or poor computation capabilities [47].

- Finally, for population states belonging to the interior of the simplex Δ, the modified pairwise comparison protocol $\rho_{ij} = \frac{[f_j(\mathbf{p}) - f_i(\mathbf{p})]_+}{p_i}$ leads to the *projection dynamics*, which are described by

$$\dot{p}_i = \sum_{j=1}^{n} \big(f_i(\mathbf{p}) - f_j(\mathbf{p})\big), \text{ for all } i \in \mathcal{S}. \tag{6}$$

Lahkar and Sandholm introduced the projection dynamics in 2008 [48]. These dynamics are derived by means of geometrical considerations. In fact, the general expression of the projection dynamics is given by $\dot{\mathbf{p}} = \Pi_{T\Delta(\mathbf{p})}(\mathbf{f}(\mathbf{p}))$, where the right-hand-side term denotes the orthogonal projection of the payoff vector onto the tangent cone of Δ at $\mathbf{p}$. In the interior of the simplex Δ, this orthogonal projection is given by (6).

Distributed Population Dynamics

According to the *mean dynamics* in (2), it is needed to know the entire population state and all the payoff functions to compute the changes of the proportion of individuals playing the ith strategy. Thus, population dynamics derived from (2) require full information to evolve. Nevertheless, in a large number of scenarios, full-information dependency is undesirable (due to, for instance, privacy issues, size of systems, limitations on the communication infrastructure, among others). In this situation, the procedure reported in [44] can be employed to relax the full-information dependency of the classic population dynamics. Before introducing this procedure, the following assumptions are required.

Assumption 1: Let $\mathcal{G} = \{\mathcal{S}, \mathcal{E}\}$ be the graph that describes the strategy-constrained interactions of a population. Let $\mathbf{p}_{\mathcal{N}_i} \in \mathbb{R}_{\geq 0}^{|\mathcal{N}_i|+1}$ be a vector formed by the elements of the set $\{p_j : j \in (\mathcal{N}_i \bigcup \{i\})\}$, where $\mathcal{N}_i$ is the set of strategies that can interact with the ith strategy following the graph $\mathcal{G}$, that is, $\mathcal{N}_i = \{j \in \mathcal{S} : (i, j) \in \mathcal{E}\}$. The payoff function associated with the ith strategy only depends on $\mathbf{p}_{\mathcal{N}_i}$. To make explicit this dependence, the payoff function is

written as $f_i(\mathbf{p}_{\mathcal{N}_i})$.

Assumption 2: Let Assumption 1 hold. The conditional switch rate ρ_{ij} only depends on the payoffs $f_i(\mathbf{p}_{\mathcal{N}_i})$, $f_j(\mathbf{p}_{\mathcal{N}_j})$ and on the proportions p_i, p_j. To make explicit this dependence, the conditional switch rate is written as $\rho_{ij}\big(f_i(\mathbf{p}_{\mathcal{N}_i}), f_j(\mathbf{p}_{\mathcal{N}_j}), p_i, p_j\big)$.

The core of the framework developed in [44] to relax full-information dependency lies on the mean dynamics for populations with strategy-constrained interactions. Since this kind of interactions can be described by a graph $\mathcal{G} = \{\mathcal{S}, \mathcal{E}\}$ and provided that Assumptions 1 and 2 are satisfied, the corresponding mean dynamics are given by

$$\dot{p}_i = \sum_{j \in \mathcal{N}_i} p_j \rho_{ji}\big(f_j(\mathbf{p}_{\mathcal{N}_j}), f_i(\mathbf{p}_{\mathcal{N}_i}), p_j, p_i\big) - p_i \sum_{j \in \mathcal{N}_i} \rho_{ij}\big(f_i(\mathbf{p}_{\mathcal{N}_i}), f_j(\mathbf{p}_{\mathcal{N}_j}), p_i, p_j\big), \text{ for all } i \in \mathcal{S}.$$
(7)

Notice that to compute $\dot{x}_i$ using (7), it is only required to know information associated with the portions of population playing neighboring strategies. Hence, applying a revision protocol that satisfies Assumption 2 in the mean dynamics for populations with strategy-constrained interactions leads to obtain population dynamics that only use local information to evolve, that is, *distributed population dynamics*. For instance, if the pairwise proportional imitation protocol $\rho_{ij} = p_j[f_j(\mathbf{p}_{\mathcal{N}_j}) - f_i(\mathbf{p}_{\mathcal{N}_i})]_+$ is considered, then the following distributed replicator dynamics are obtained

$$\dot{p}_i = p_i \left(f_i(\mathbf{p}_{\mathcal{N}_i}) \sum_{j \in \mathcal{N}_i} p_j - \sum_{j \in \mathcal{N}_i} p_j f_j(\mathbf{p}_{\mathcal{N}_j}) \right), \text{ for all } i \in \mathcal{S}.$$
(8)

In the same way, the pairwise comparison protocol generates the distributed Smith dynamics that are given by

$$\dot{p}_i = \sum_{j \in \mathcal{N}_i} p_j \left[f_i(\mathbf{p}_{\mathcal{N}_i}) - f_j(\mathbf{p}_{\mathcal{N}_j}) \right]_+ - p_i \sum_{j \in \mathcal{N}_i} \left[f_j(\mathbf{p}_{\mathcal{N}_j}) - f_i(\mathbf{p}_{\mathcal{N}_i}) \right]_+, \text{ for all } i \in \mathcal{S}.$$
(9)

Properties of Population Dynamics

Population dynamics exhibit appealing features that can be exploited in engineering applications. This section presents two fundamental properties of population dynamics: the invariance of the simplex Δ in (1), and the convergence of the trajectories of population dynamics towards the Nash equilibria.

Simplex Invariance

In previous works such as [49], [13], it has been shown that the population mass m is conserved over time under population dynamics. Furthermore, it has been proved that the population state $\mathbf{p}$ remains nonnegative for these dynamics. Therefore, the simplex Δ is invariant. This property is formalized in Lemma 1.

Lemma 1: **Simplex Invariance**. Let Δ be the simplex given in (1). If $\mathbf{p}(0) \in \Delta$, then $\mathbf{p}(t) \in \Delta$, for all $t \geq 0$ under both the standard mean dynamics (2) and the mean dynamics for populations with strategy-constrained interactions (7).

Proof: A proof of this lemma can be found in [49], [13], [44]. The idea behind the proof is sketched follows: first, mean dynamics satisfy mass conservation because they do not admit neither birth nor elimination of individuals. Indeed, changes in the population appear due to

switching of players among strategies. Second, mean dynamics guarantee nonnegativeness of the population state. This property follows from the fact that, under mean dynamics, the fraction of individuals playing strategy i only decreases due to switching of individuals to other strategies. Therefore, if this fraction is null, migration is not possible. ∎

Remark 1: Notice that, since all population dynamics are based on the standard mean dynamics (2), it is possible to conclude that any class of population dynamics satisfies simplex invariance. The same condition holds for the distributed population dynamics because they are based on the mean dynamics for populations with strategy-constrained interactions (7). ◇

According to Lemma 1 and the definition of the simplex Δ given in (1), population dynamics satisfy both mass conservation and nonnegativity of the elements of the population state $\mathbf{p}$. To illustrate this result, consider the classic *rock-paper-scissors* game, for details of this game see "*Rock-paper-scissors* game in a population with different types of interactions". Figure 2 shows the trajectories of a population that is evolving according to the replicator dynamics (Figure 2(a)) and Smith dynamics (Figure 2(b)). Notice that both replicator and Smith dynamics keep the trajectories in the interior of the simplex Δ.

The property stated in Lemma 1 is crucial in many applications of population dynamics, especially in those related to optimization and control, where the invariance of the simplex Δ guarantees the satisfaction of a given constraint or even a set of constraints (see [44], [27], [26]).

Convergence to Nash Equilibria

Other key property of population dynamics is that, under some conditions, they evolve towards the Nash equilibria of the corresponding population game. Although convergence conditions cover several types of population games, this article focuses on full-potential games since they may model a broad class of engineering applications; for instance, access control in communication networks [22], bandwidth allocation [25], hierarchical frequency control in microgrids [26], dispatch of electric generators [27], and so forth.

Before introducing the result on convergence to Nash equilibria, the definition of a full-potential game is introduced.

Definition 3: **Full-Potential Game** (adapted from [13]). Let $\mathbf{f} : \mathbb{R}^n_{\geq 0} \mapsto \mathbb{R}^n$ be a payoff vector that characterizes a population game with payoffs defined on the positive orthant. If there exists a continuously differentiable potential function $V : \mathbb{R}^n_{\geq 0} \mapsto \mathbb{R}$ that satisfies $\nabla V(\mathbf{p}) = \mathbf{f}(\mathbf{p})$, for all $\mathbf{p} \in \mathbb{R}^n_{\geq 0}$, then $\mathbf{f}$ is a full-potential game. ◇

Roughly speaking, a full-potential game is a game whose payoff vector is equal to the gradient of a potential function. Given a full-potential game, Theorems 1 and 2 establish conditions for guaranteeing the convergence of the population state to Nash equilibria under different population dynamics.

Theorem 1: If $\mathbf{f}$ is a full-potential game with strictly concave potential function, $\mathbf{f}$ has a unique Nash equilibrium $\mathbf{p}^*$. Moreover, if $\mathbf{p}(0) \in \text{int}\Delta$, where $\text{int}\Delta = \left\{ \mathbf{p} \in \mathbb{R}^n_{>0} : \sum_{i=1}^{n} p_i = m \right\}$, then $\mathbf{p}(t)$ asymptotically converges to $\mathbf{p}^*$ under replicator dynamics, Smith dynamics, and projection dynamics.

Proof: A proof of this theorem can be found in [13]. It is worth noting that replicator dynamics have other equilibrium points different from the Nash equilibrium of the game. However, these equilibrium points are not stable. ∎

As shown in Theorem 2, a similar result is obtained for distributed population dynamics.

Theorem 2: Let **f** be a full-potential game with strictly concave potential function. Furthermore, assume that the unique Nash equilibrium of the game $\mathbf{p}^*$ belongs to the interior of the simplex Δ, that is, $\mathbf{p}^* \in \text{int}\Delta$. If $\mathbf{p}(0) \in \text{int}\Delta$ and the graph that describes the strategy-constrained interactions among the individuals of the population is connected, then $\mathbf{p}(t)$ asymptotically converges to $\mathbf{p}^*$ under both the distributed replicator dynamics and the distributed Smith dynamics.

Proof: A proof of this theorem can be found in [44]. ∎

Summarizing, under appropriate initialization, convergence to Nash equilibria is guaranteed for full-potential games whose potential function is strictly convex. In the case of distributed population dynamics, additional conditions are required. These conditions are related to the location of the Nash equilibrium inside the simplex Δ, and the connectivity of the graph that models the strategy-constrained interactions of the individuals within the population.

Convergence properties of population games have been exploited in engineering applications during the last few years (see [29], [30] and references therein). This fact is mainly given since there exists an equivalence between the Nash equilibria of a full-potential game and the arguments that maximize its potential function. Figure 3 illustrates this property by showing the convergence of the population state (whose evolution is depicted in black solid line) to the Nash equilibrium of a full-potential game under replicator dynamics and distributed replicator dynamics. Notice that the Nash equilibrium matches the argument that maximize the potential function.

In conclusion, if the payoff vector is selected in a proper way, that is, as the gradient of an objective function $V(\mathbf{p})$, population dynamics become a constrained optimization method where the constraint is given by the simplex Δ. Indeed, this feature has been employed in recent research, such as in [50], [27]. In this works, the authors seek to maximize certain criteria subject to the simplex constraint, which represents a resource restriction in most of the considered engineering problems. Besides, it is worth noting that the application of population dynamics is not limited to static optimization. Indeed, these dynamics have been used to design time-varying adaptive controllers based on extremum seeking architectures [29], [25]. Once the preliminary concepts of population dynamics have been introduced as well as the properties exhibited by these game-theoretical approaches, three applications within the context of smart cities are presented and discussed. The control design for the three aforementioned applications is addressed by using the population dynamics while exploiting their stability and invariance set properties.

Engineering Applications

Lighting Systems

One of the main tasks in building automation is the efficient use of energy resources due to the high building consumption, which is around 70% of the electricity produced in developed countries [51]. In particular, lighting systems account for a significant energy usage with a 25% and a 12% in commercial and residential sectors, respectively [52], representing about 7% of the global CO_2 emissions by the flaring of fossil fuels to produce electricity [53].

Modern lighting has a large potential for energy savings using different strategies such as occupancy sensors, daylighting, and other control and regulation systems, decreasing consumption between 24% to 38% [54]. However, since illumination is related to people welfare

and productivity, appropriate lighting controllers must also provide comfortable and uniform lighting levels in the environment. Recent developments in efficient lamps, dimmable actuators, light sensors, wireless communication devices, and reduced embedded controllers allow designing distributed strategies to deal with the challenges of new lighting systems.

Lighting control techniques cover a wide range of applications, from conventional methods to advanced implementations of intelligent techniques and agent-based controllers [55], where the suitable use depends on the environment features. In this sense, advances in building designs and networked sensor-actuator systems have motivated the development of techniques based on hierarchical structures [56], systems with novel decentralized integral controllers [57], and wireless sensors with optimization algorithms [58], to deal with the energy efficiency and provide comfort to the occupants.

The implementation of successful control strategies in large systems, such as office buildings, requires the division of the environment in zones with local controllers acquiring and processing information in a communication network. When the number of sensors and actuators increase, most of the centralized techniques become inefficient, while distributed strategies with limited information are robust to packet loss while reducing the computational cost of the control techniques [59]. To control the illuminance in large-scale systems, it is presented and discussed a resource allocation strategy based on the distributed replicator dynamics to obtain desired illumination levels, taking into account a limited amount of energy and the network topology defined by the local exchange of information among the controllers. This methodology is applied in the experimental testbed reported in [57] to show the appropriate management of cross-illuminance, daylighting, and energy saving.

Modeling light-propagation effects to calculate the illuminance at each point of an environment is a complex task that is usually performed by using specialized software tools [60]. Nevertheless, the room conditions are relaxed here assuming the lamps as punctual light sources and small area sensors. Besides, assuming that the light emission of each lamp has the same intensity in a broad solid angle (as in incandescent or fluorescent lamps) and that the sets lamp-ballast are fully dimmable, the illuminance perceived by the ith sensor due to the jth lamp can be expressed by

$$E_{ij} = \frac{k_j v_j}{d_{ij}^2},$$

where v_j is the voltage applied to the lamp j, d_{ij} is the distance between the ith sensor and the jth lamp, and k_j is a positive constant depending on the lamp characteristics (luminous efficiency and effective illuminance solid angle, among others [61]). Then, different cross-illuminance conditions can be obtained by modifying k_j. The total illuminance measured in the ith zone of a room split into n zones is given by

$$E_i(p) = \sum_{j=1}^n E_{ij} = \sum_{j=1}^n \frac{k_j v_j}{d_{ij}^2}. \tag{10}$$

The illuminance at each zone depends on all the voltages applied to the lamps. This condition makes the resource allocation problem difficult since changes in a certain voltage affect directly all the output variables.

On the other hand, the system communication network is modeled by an undirected graph $\mathcal{G} = (\mathcal{V}, \mathcal{E})$, where the node set $\mathcal{V}$ is given by local controllers at each lighting zone, and the edges set $\mathcal{E}$ is given by the communication links for bidirectional information exchange.

Lighting Control

To obtain a desired illumination in a lighting system with n zones, the resources to be managed are the voltages applied to the lamps. Therefore, according to the population-game theory (Table 1), the population state is analogous to the voltage vector $\mathbf{v} = [v_1 \; v_2 \; \ldots \; v_n]^\top$, the strategy set is given by the illumination zones, and the population mass is the limited voltage (or power) available in the system, which is denoted as $V_{tot} > 0$. Besides, given the communication constraints, an appropriate distributed control can be performed by the distributed replicator dynamics described in (8).

However, the invariance of the simplex Δ is not an advantage in this case. With this property, if $\mathbf{v}(0) \in \Delta$ then

$$\sum_{i=1}^{n} v_i = V_{tot}$$

is ensured for all time. Notice that even when V_{tot} is large and the setpoints are small (references are achieved with only a portion of the total resources), V_{tot} is still split among the n lamps. In consequence, the setpoints cannot be reached and the appropriate resource constraint is

$$\sum_{i=1}^{n} v_i \leq V_{tot}. \tag{11}$$

To solve this problem, a *fictitious zone* is added to the lighting environment to act as a surplus variable in the resource allocation. It is worth noting that the remaining power is not applied to any lamp and the desired illumination is obtained only with the required voltage. Then, an extended population state $\mathbf{p_{add}} \in \mathbb{R}_{\geq 0}^{n+1}$ is defined as

$$\mathbf{p_{add}} = [p_1 \; p_2 \; \ldots \; p_n \; p_{n+1}]^\top,$$

and the simplex

$$\Delta_{add} = \{\mathbf{p_{add}} \in \mathbb{R}_{\geq 0}^{n+1} : \mathbb{1}_{n+1}^\top \mathbf{p_{add}} = m\}$$

is still invariant under the dynamics in (8) with the addition of a new strategy to the game [50]. However, the network topology must be also modified defining the augmented graph $\mathcal{G}_{add} = (\mathcal{V}_{add}, \mathcal{E}_{add})$, where $\mathcal{V}_{add} = \mathcal{V} \bigcup \{n+1\}$ and $\mathcal{E}_{add}$ is the union of the original set of edges $\mathcal{E}$ with at least one pair $(i, n+1)$ for some $i = 1, \ldots, n$. In other words, the fictitious zone is attached to the original network with links to real nodes to preserve the connectedness of the new graph.

With these conditions, the required constraint (11) is now satisfied. Moreover, the equilibrium point for the extended dynamics is the same defined by the payoff equality (including the fictitious zone)

$$f_i^* = f_j^*, \text{ for all } i, j \in \mathcal{V}_{add}. \tag{12}$$

Taking advantage of this property, the control goal for the lighting system is achieved if the payoff functions are defined depending on the tracking error between the illuminance measured in each zone (E_i) and the setpoint (E_{set_i}). Then, the payoffs are given by

$$f_i = B + E_{set_i} - E_i, \text{ for all } i = 1, \ldots, n \tag{13}$$

$$f_{n+1} = B, \tag{14}$$

where $B > 0$ is a large enough constant to guarantee that $f_i > 0$, satisfying the payoff conditions in biological population dynamics. Therefore, at the equilibrium, $f_i^* = B$, and the tracking error becomes zero at each zone ($E_{set_i} - E_i^* = 0$, for all i). Notice that the definition of the payoff function in the fictitious zone determines the equilibrium value of the rest of payoffs and allows the distributed replicator dynamics to obtain the desired illuminances. It is also remarkable that the achieved steady state is the unique Nash equilibrium according to the properties of the replicator dynamics [49], taking into account surplus resources, decreasing payoff functions, and connected graphs for the resource allocation process.

In most application cases of evolutionary game theory [49], as well as in behavioral ecology [62], the payoffs of the players are decreasing to ensure stability of the equilibrium points, that is, the more individuals sharing the same strategy, the smaller the payoff. In the lighting model, if the illuminance E_i in (10) is replaced into (13), the real payoffs fulfill this requirement. Besides, with certain conditions over the environment and appropriate initial conditions ($\mathbf{p_{add}}(0) \in \Delta_{add}$), the asymptotic stability of the equilibrium point (12) is demonstrated in [50] with a locally-Lipschitz Lyapunov function.

Testbed Application Cases

The application of the designed strategy is shown in two different environments of the testbed in "An experimental testbed for lighting systems".

Divided Environment: The control objective in this case is to obtain a uniform illuminance for all zones ($E_{set_i} = E_{set}$, for all $i = 1, 2, \ldots, 8$). To show the influence of the communication network, two topologies are chosen to indicate the information exchange among local controllers (including the fictitious zone denoted by FZ). The extended graphs ($\mathcal{G}_{add}$) for the application of the distributed replicator dynamics are presented in Figure 11. It is worth remarking that the fictitious zone does not represent a real controller in the system, but some extra software tasks in one of the controllers where the FZ is attached to. Nevertheless, a communication channel is needed between the nodes with links to FZ (if there exists already a link, no modifications are required in the original network).

Figure 12 presents the results of the control process. Dashed and solid lines for cases 1 and 2, respectively, show the behavior of the measured illuminance in each sensor (right axis and black lines), and the voltage applied to each lamp (left axis and blue lines). The setpoint (red-dotted line) is achieved in all the zones after an initial transient period, according to the expected results. Given that zones are uneven, the required power at each lamp is different in order to obtain the uniformity in the environment.

To simulate the influence of the daylight, in $t = 40$ s an external light is applied to the environment through a window close to zones 7 and 8 (see Figures 12(d), and 12(h)). It is shown that the resources are reallocated to react against the disturbance and to reach again the setpoint. Voltages applied to the lamps are reduced taking advantage of the daylighting, representing better use the available resources and energy savings. Notice that the reduction on the necessary power to maintain the desired illuminance is significant and zones 7 and 8 are the most affected by the disturbance. At $t = 60$ s, the window is closed and the correction on lamp voltages allows the system to achieve again the setpoint.

The closeness of the fictitious zone to certain nodes influences the transient behavior. In the first case, zones 7 and 8 presented in Figures 12(d) and 12(h), respectively, reach the equilibrium point faster than the farther zones, while in the second case, zones 1 and 8 are the

fastest ones. With the definition of the payoff in FZ, this node has relevant information about the equilibrium state. Therefore, closer zones need less time to access this data across the network and their dynamics are faster.

Open Environment: The uneven cross-illumination effects are enhanced in this environment and the high variable couplings represent a more challenging control problem with interesting results. The desired reference in this case changes from $E_{set} = 6$ V (during the first 100 s) to $E_{set} = 5$ V (from $t = 100$ s to $t = 200$ s), and finally it is set to $V_{set} = 5.5$ V for the last 100 s. As in the divided environment, all zones have the same illuminance setpoint and the network topologies are given by the graphs shown in Figure 11.

Results for the first topology are presented using dashed lines in Figure 13. Although the total power resources are enough, the desired tracking is only achieved in zones 7 and 8 (see Figures 13(d) and 13(h)), which are connected to the fictitious zone. In the rest of zones, the illuminance does not reach the setpoints. It is remarkable that even though the voltages applied to the lamps 5 and 6 drop to zero (see Figures 13(c), and 13(g)), their illuminance is higher than the desired setpoint. This absence of resources in certain zones is known as *truncation* [62] and, in population-games terms, represents strategies with no population shares. Taking into account the network topology, these truncated zones are nodes whose participation in the information exchange is depleted and, in consequence, the graph may become disconnected. This situation is illustrated in Figure 14(a), where the truncation of nodes 5 and 6 splits the graph into two separated components.

The truncation in central zones allows the position of the fictitious zone to determine the connectivity of the graph, which is a necessary condition to perform the resource allocation process [63]. For instance, in the network topology for case 2 (Figure 14(b)), the resulting graph is still connected due to the attachment of FZ. In consequence, as it is shown using solid lines in Figure 13, all untruncated nodes achieve the setpoints since the resource allocation is performed over the resulting graph including all zones (except the truncated ones). However, due to the cross-illumination effects, the illuminance in zones 5 and 6 is high even when their lamps are turned off.

With the distributed replicator strategy, the light influence among zones provides an opportunity to save energy taking into account a robust network topology to avoid the formation of insulated components in the graph. Therefore, the location of the fictitious zone is a key factor for the graph robustness given that the connections of this new node affect the graph topology. Hence, defining the neighborhood of FZ becomes a design parameter that may connect different components in a room, distant environments such as different floors in buildings, or increase the connectedness in weak graph topologies.

Smart Grids

The potential of the population dynamics approach for solving a fundamental problem that arises in smart grids is now presented and discussed. In particular, the optimal dispatch of active power of distributed generators (DG) is solved as a dynamic resource allocation problem. Conventional dispatch problem in power systems consists in minimizing the total generation cost or in maximizing the total utility of all generators, while the restrictions on power balance and generation capacity are satisfied [41]. Here, the maximization of utility functions is adopted. Traditionally, the economic dispatch problem has been solved by static optimization algorithms [42], or direct search methods [43], which operate off-line in a time interval between five minutes

to one hour [37]. However, changing environments need new control tools for the management of distribution systems.

The solution of the optimal dispatch of active power of distributed generators as a dynamic resource allocation problem based on population dynamics is first presented in [27] in the context of microgrids. In this context, a microgrid is defined as a set of interconnected distributed devices, for example generators and loads, which must cooperate with other elements in the electric network to be collectively treated by the grid as a controllable load or generator. First, it is considered the case where the dispatch algorithm is being executed at the central controller of the microgrid. Then, a distributed version of the algorithm is presented, where the dispatch algorithm is executed in a fully-distributed fashion at each distributed generator.

Dynamic Economic Dispatch Algorithm for Microgrids

A hierarchical dynamic management strategy is presented to deal with the main control issues related with microgrids. Two control levels are considered. At the lower level of the microgrid architecture, distributed generators connected to loads through an inverter are found. The distributed generators are modeled as controllable voltage source inverters. The magnitude and frequency of the output voltage are controlled by means of a droop-gain controller [64]. For more details about this approach the reader is referred to [26] and references therein. An illustrative general scheme is presented in Figure 15 for a microgrid with seven distributed generators (DG 1, DG 2, ..., DG 7) and several loads connected in a electrical topology adapted from the IEEE 30-bus distribution system.

At the higher level of the microgrid control architecture, it is designed a control strategy that dynamically dispatches active power setpoints. This controller has to generate the power setpoints based on economic criteria. In this model, the production costs of active power and load demands are considered as external inputs coming from the lower level control to the microgrid central controller, where the dynamic dispatch based on replicator dynamics is being executed. This fact implies that costs and load demands could be time-varying, allowing the inclusion of renewable energy resources. The main focus here is on the higher level of the microgrid, where the dynamic dispatch is executed. The maximization of utility functions for the economic dispatch problem is adopted including active power generation by means of voltage source inverter connected to distributed generators at a lower level. The economic dispatch problem (EDP) can be formulated as follows

$$\max J(\mathbf{p}) = \sum_{i=1}^{n} J_i(p_i),$$

such that

$$\sum_{i=1}^{n} p_i = \sum_{i=1}^{n} l_i = P_D,$$

$$0 \leq p_i \leq P_{max_i}, \quad \text{for all} \quad i = 1, 2, ..., n,$$

(15)

where p_i is the power setpoint for the ith DG, n is the number of DGs, l_i are the loads, P_D is the total load demanded by the microgrid, P_{max_i} is the maximum generation capacity of the ith DG, and $J_i(p_i)$ is the utility function of each DG. This utility function must be defined according with the economic dispatch criterion [41], which states that all generation units must operate at

the same marginal utilities, that is,

$$\frac{dJ_1}{dp_1} = \frac{dJ_2}{dp_2} = \cdots = \frac{dJ_n}{dp_n} = \lambda, \tag{16}$$

for some $\lambda > 0$ such that $\sum_{i=1}^n p_i = P_D$. Based on the economic dispatch criterion (16), this optimization problem can be solved using quadratic utility functions for each DG [27].

Population-Games Approach for Dynamic Dispatch in Microgrids

The population dynamics chosen in this work to deal with the EDP are the replicator dynamics (3). The replicator dynamics is used to solve the EDP as a resource allocation problem. Basically, n is defined as the total number of generators in the system and the ith strategy corresponds to choose one of the n DGs in the microgrid. Each p_i is the amount of power assigned to each DG, and it corresponds to the proportions of individuals that choose the ith strategy in $\mathcal{S}$. To achieve an appropriate performance in steady state, the load demanded power (P_D) should be the sum of all power set-points, that is, $\sum_{i=1}^n p_i = P_D$. To guarantee the power balance, the results presented in [65] are used, where the choice of $\bar{f} = (1/P_D) \sum_{i=1}^n p_i f_i$ guarantees the invariance of the constraint set Δ in (1).

This result ensures that if $\mathbf{p}(0) \in \Delta$, then $\mathbf{p}(t) \in \Delta$, for all $t \geq 0$. In other words, the control strategy defines setpoints such that they guarantee the suitable balance between demanded power and generated power by the DGs for all $t > 0$. This condition produces, in steady state, a frequency deviation equal to zero and, in consequence, an adequate frequency regulation. In order to include economical and technical criteria into the control strategy, the power dispatched to each generator depends on a cost factor and the maximum power generation. An important characteristic of the replicator dynamics is that its stationary state is achieved when the payoff functions are all equal to the average payoff $\bar{f}$. This condition is the link between replicator dynamics and the EDP, since it is equal to the economic dispatch criterion (16) choosing the payoff function to be

$$f_i(p_i) = \frac{dJ_i}{dp_i}, \quad \text{for all} \quad i = 1, 2, ..., n. \tag{17}$$

Based on the economic dispatch criteria (16), which guarantee that the solution is optimal while satisfying the constraints, these optimization problems can be solved using payoff functions as marginal utilities based on the fact that all payoff functions are equal to $\bar{f}$. The selected payoff is a function that increases (decreases) when the power is far (near) from (to) the desired setpoint. In this form, the replicator allocates more (less) resources to those generation that have a payoff that is above (below) the average. This behavior can be modeled using a logistic-type function [66]. In general form,

$$f(y) = ry\left(1 - \frac{y}{K}\right),$$

where y is the independent variable, and K is a parameter known as the carrying capacity such that $y \in (0, K)$. The particular payoff functions related to the EDP use as parameters the nominal power (as carrying capacity) and a generation cost factor (c_i) of each DG. Then, according to (17), the payoff functions of each DG are defined as

$$f_i(p_i) = \frac{dJ_i}{dp_i} = \frac{2}{c_i}\left(1 - \frac{p_i}{P_{max_i}}\right), \quad \text{for all} \quad i = 1, 2, ..., n. \tag{18}$$

In addition, the fact of using all payoff functions as marginal utilities leads the population game to be a potential game, which implies that Nash equilibria correspond to the Karush-Kuhn-Tucker first-order necessary conditions [67]. The payoff functions in (18) lead to the following quadratic utility functions for each DG in the optimal dispatch problem [27]

$$J_i(p_i) = \frac{1}{c_i} \left(2p_i - \frac{p_i^2}{P_{max_i}} \right), \quad \text{for all} \quad i = 1, 2, ..., n. \tag{19}$$

On the other hand, if (3) is taken in steady state, that is $\dot{p}_i = 0$, and $p_i > 0$, the equilibrium point is an optimal point for the resource allocation related to a wide family of payoff functions [68]. This payoff function has been used in several works such as [27], [26], [69], among others.

Distributed Replicator Dynamics for Optimal Dispatch

The dispatch algorithm presented previously requires a centralized controller with a high-bandwidth communication infrastructure as the number of nodes increases to handle information from every single node along the distribution system. Therefore, distributed control algorithms are becoming promising approaches in the context of smart grids since they can be more robust and resilient to network variations. The replicator dynamics equation needs full information from all the agents to calculate $\bar{f}$. The replicator dynamics can be understood as a multi-agent controlled system, where each agent dynamics are described by (3), and the controller that receives the state information of all agents is given by the average payoff. It has been assumed that the communication between agents and the controller is ideal and that full information is available, which sometimes in real implementations is not possible due to limitations induced by the communication network. However, replicator dynamics as a network control system have been shown independent of delays [70]. In addition, in [67] it is suggested that contractive games admit global convergence results under evolutionary dynamics. To analyze the effects of the communication infrastructure in the optimal dispatch algorithm, it has been proposed a distributed version of the replicator dynamics algorithm to respond dynamically to the needs of the microgrid assuming that no full information is available. A distributed replicator dynamics to dispatch distributed generator over a communication topology in a microgrid is proposed based on (8). The distributed replicator dynamics consider local information from the neighbors of a given agent in an interaction network. In order to guarantee that the related optimization problem can be solved, Assumptions 1 and 2 are considered.

Assumption 1. The communication graph between generation units is undirected and connected.

Assumption 2. The Nash equilibrium $\mathbf{p}^*$ belongs to the interior of the simplex Δ.

Assumption 1 implies that all generators are communicated. A neighborhood of agents are necessary to calculate a local payoff function for each generator. Assumption 2 is related to the problem feasibility. If the demand is lower than the capacity of the generators, then it means that the total capacity of power generation is inside the simplex and the solution of the optimization problem can be found. On the other hand, since the utility functions are concave then the solution of the problem is unique. In addition, in steady state the balance condition is satisfied.

The full-information constraint for the average payoff is modified to include the communication graph between the generators. A communication infrastructure with limited message passing can be effectively used among the multi-agent system. To guarantee the power

balance, the results presented in [71] are used, where it is proven the invariance of the constraint set Δ. The full-information constraint for the calculation of the original average payoff is relaxed and the distributed replicator dynamics equation can be used to satisfy the network constraints in the general EDP given by the topology of the graph. Some additional features of the distributed replicator dynamics can be discussed. First, the steady state of (8) is achieved when

$$f_i(p_i^*) \sum_{j \in \mathcal{N}_i} p_j^* = \sum_{j \in \mathcal{N}_i} f_j(p_j^*)p_j^* \quad \text{for all } i = 1, \ldots, n, \tag{20}$$

which is satisfied if $f_i(p_i) = f_j(p_j^*)$, for all $j \in \mathcal{N}_i$ and all i. Considering that Assumption 1 holds, the following condition is satisfied

$$f_i(p_i^*) = f_j(p_i^*) = \bar{f}^*, \tag{21}$$

where $\bar{f}^*$ is the equilibrium average payoff. Then, at steady state all payoff functions are equal and all individuals earn the same payoff. Hence, the distributed replicator dynamics equation and the replicator dynamics equation have the same equilibrium point $\mathbf{p}^*$. On the other hand, the coverage of the total demand is respected because the set Δ is also invariant under the distributed replicator dynamics equation. This property has been proved in [71] using some topological properties of the connected graphs to show that $\sum_i \dot{p}_i = 0$ when $\mathbf{p}(0) \in \Delta$. With this property, it is ensured that the demanded power P_D is supplied by the DGs in the dispatch process.

Considering that (20) is only a possible condition to satisfy (21), a stability analysis of this equilibrium point is required to show the convergence from any $\mathbf{p}(0) \in \Delta$ to the point of maximum utility $J(\mathbf{p}^*)$. The main stability result has been recently presented in [71] as a proposition, which states the general payoff functions conditions to guarantee the convergence of the method.

Proposition 1 ([71]): If f_i is a strictly decreasing locally Lipschitz function, $\sum_{i=1}^{n} P_{max_i} \geq P_D$, $\mathbf{p}(0) \in \Delta_p$, and $f_i(p_i) > 0$ for all $0 \leq p_i \leq P_{max_i}$, then the equilibrium point $\mathbf{p}$ satisfying (21) is asymptotically stable in Δ under the distributed replicator dynamics (8). According to the payoff definition in this specific application, the equilibrium point of (8) is maximizing the utility functions in the system.

Simulation Results for the Dynamic Dispatch Algorithm

The dynamic economic dispatch algorithm based on distributed replicator dynamics (8) is tested here for a low voltage microgrid case study of seven distributed generators with several loads connected in a electrical topology adapted from the IEEE 30-bus distribution system [41]. An unpredicted increase in the total demand is activated at $t = 0.8$ s. This unpredicted load can take negative values and can be considered as a non-dispatchable DG or intermittent renewable resource. The microgrid test system is shown in Figure 15 (a) with total power demand $P_D = 9$ kW, an unpredicted load increase of 3 kW, and different costs for each generator with DG 7 as the more expensive and with DG 3 as the cheapest. DG 1, DG 4, DG 5, and DG 6 are similarly expensive, while DG 2 is cheaper. The microgrid is started from zero initial conditions and is operating at a frequency of 60 Hz. The capacity of generators DG 1, DG 2, DG 3, DG 4, DG 5, DG 7 is 3.6 kW ($P_{max_{1,2,3,4,5,7}} = 3.6$ kW), and the capacity of generator DG 6 is 2 kW ($P_{max_6} = 2$ kW). Figure 15 (b) shows the topology of the communication network between the DGs. It has been considered that through this topology the DGs interchange information about

the dynamic power dispatch of each DG.

The control inputs have been calculated using a Matlab/Simulink model using SimPower on a Core i7 laptop with 4Gb RAM. Figure 16 (a) shows that the frequency of the microgrid is maintained between an operational interval (less than $+/-0.2$ Hz) all the time since the power balance is kept at a minimum and the response of the distributed replicator algorithm is dynamic and continuous. It can be observed when an increment in load at $t = 0.8$ s is made and the frequency has a small variation but stabilize to zero again. In Figure 16 (b) is shown the power dynamically dispatched for each generator. It can be observed that, at the beginning, generator DG 7 (more expensive) is dispatched to a minimum power during the low demand intervals due to the high generation cost, while the generator DG 3 (cheapest) is dispatched near to its maximum capacity and remains near that value despite load variations. However, when the demand is increased at $t = 0.8$ s, generator DG 7 increases its power to compensate the increased demand. It is also noticed that due to less capacity the expensive DG 6 reaches its maximum capacity at the load variation. Finally, it is shown that DGs with similar parameters have similar responses, as it is the case of DG 1, DG 4, DG 5, and DG 6. DG 2 is dispatched near to its maximum capacity since it is a cheap generator.

Urban Drainage Systems

Urban Drainage Systems (UDS) are large-scale systems composed of arrangements of channels connected by chambers, which transport wastewater, stormwater, or both. These elements may be represented by interconnected reservoirs able to store wastewater, that is, elements that store wastewater within the UDS may be grouped and simplified as a unique reservoir for control purposes as made with the concepts of virtual tanks in [72]. Besides, the chambers composing the UDS may be of inspection and/or collection. The efficiency of the UDS is given by their capacity to perform under specific design conditions along the time. For instance, some specific design conditions are the average velocity, the Froude number, the filling ratio, among others [73]. In order to meet these design conditions, UDS are regulated by using measurements collected by proper equipment and also using knowledge about the control structures; for instance, retention gates as presented in [72]. Regarding the structure topology of UDS, these systems might be commonly characterized by a tree topology (or also known as dendritic) [74]. Under this specific type of topology, clusters of channels in the UDS converge to a unique drain point. Moreover, each cluster is known as a stage within the whole system.

Broadly speaking, the UDS can be modeled by using either an hydrological or hydraulic approach. The hydraulic model is mainly based on physics. For instance, the Navier-Stokes equations, or their particular well known case, the one dimentional Saint-Venant equations [75]. On the other hand, the hydrological model is mainly based on the mass conservation principle, and it is also considered as an hydraulic model simplification. Even though the hydrological models are not accurate for transient processes, these models are useful to characterize the distribution of flows along the UDS and coming from exogenous non-manipulated sources or events. Besides, the hydrological models do not demand high computational costs in comparison with the hydraulic models, which is a relevant aspect when designing real-time control, but might be a relevant source of uncertainty for both the evolution and management of the system.

Furthermore, computational burden is a quite relevant aspect taking into account that the UDS are large-scale systems involving a large number of states and control inputs that have to be computed in a limited time, for instance, it is expected that a centralized controller requires

more time than a non-centralized controller computing less number of control inputs.

One of the main control objectives considered for large-scale UDS is the minimization of overflows, that is, fluids released to the receptor environment and/or streets. To this end, it is used to solve a resource allocation problem at each stage that UDS have. This is made by using a decentralized population-games-based controller. Consequently, due to the fact the controller is in charge of managing fluids, a flow-based hydrological model is appropriate to characterize the behavior of the system from the control-oriented point of view. Finally, it is also contemplated that rain events might occur unexpectedly along the time. Therefore, rain events are treated as UDS disturbances. The selected UDS dynamics are given by the Muskingum linear model, which is an hydrological-based model (see "Muskingum model").

System Partitioning and Control via Population Dynamics

The stated decentralized population-games-based control consists in dividing the UDS into N different sub-systems with the same local topology. The control scheme is decentralized since the different controllers for each sub-system neither interact to each other nor exchange information in order to compute the optimal control inputs. Then, a population dynamics-based controller is designed at each sub-system. This population dynamics approach has been already studied in [76] and [31] as a data-driven control approach. Prior showing the methodology to design the population-games-controller, an analogy between each element of the population dynamics approach and the elements in UDS is presented in Table 1.

Regarding the system partitioning issue –the division of the UDS into N sub-systems–, and taking into account the fact that each sub-system is controlled independently by solving a resource allocation problem with population dynamics, the criterion to define the partitions consists in finding sub-systems whose structures are given by a convergence-flow topology according to Definition 4.

Definition 4: **Flow-Convergence Topology.** This topology is composed of n reservoirs whose outflows correspond to the inflows of a common reservoir as presented in Figure 4(a) [31]. In this topology, n reservoirs with outflows converging to a common one are called *source reservoirs*, and the reservoir whose inflow is given by all the outflows from source reservoirs is called *receptor reservoir*. Notice that the topology presented in Figure 4(c) corresponds to a case of flow convergence with a single source reservoir. $\diamondsuit$

The partitioning of the UDS is performed by dividing the whole system into *cases of flow convergence*, each one of them controlled by a local population-games-based controller, that is, the entire control system for the UDS is composed of N local controllers that do not communicate with each other and which operate independently and in parallel, composing a non-centralized control topology.

In the *case of flow convergence* topology with more than one source reservoirs, the set of source reservoirs is given by $\mathcal{S} = \{1, ..., n\}$. The volume of the reservoir $i \in \mathcal{S}$ is denoted by v_i, its maximum volume capacity is denoted by $\bar{v}_i$, and its inflows and outflows are given by $q_{in,i}$ and $q_{out,i} = K_i p_i v_i$, respectively. The parameter $p_i \in [0,1]$ determines the percentage of opening of the output gate associated to the ith reservoir, and $K_i > 0$ scales the outflow, whose interpretation can be associated to a discharge coefficient of the reservoir. The volume of the receptor reservoir is denoted as v_r, and its maximum volume is denoted by $\bar{v}_r$. Besides, the control input $\mathbf{p}$ should satisfy the simplex set describing all the possible strategic distributions given by (1). Notice that, for the particular case of *flow convergence* with only one source

reservoir ($\mathcal{S} = \{1\}$ is a singleton set), the reservoir outflow is given by $p_i = m$, $i \in \mathcal{S}$.

The inflow of the receptor reservoirs are not considered to be *physically* constrained since it is assumed that their maximum possible inflows, according to the discharge coefficients and the maximum volumes of the respective source reservoirs, are supported by the infrastructure of the system. However, the inflows of the receptor reservoirs are constrained in function of the available capacity of these reservoirs. This fact allows the source reservoirs to retain wastewater if it is necessary to avoid overflows as it is explained next.

The population mass is selected to have an upper bound $m \leq \ell$, where ℓ is a design parameter. Therefore, the value for the population mass m, which determines the upper limit for the output gates percentage, varies every selected period time τ depending on the measured volume of the receptor reservoir, that is, $m = \ell \left(1 - v_r/\bar{v}_r\right)$. Notice that if ℓ is selected greater than one, then it is possible that, in the evolution of the portion of the mass of players, p_i takes values greater than one, for any $i \in \mathcal{S}$. However, since the opening percentage should belong to the interval $[0, 1]$, the control signal would be saturated because of the actuator physical constraint. Therefore, in this article it is proposed to establish the design parameter $\ell = 1$, guaranteeing that $p_i \in [0, 1]$ for any population mass $m = \ell \left(1 - v_r/\bar{v}_r\right)$.

For instance, let $m = m_1$ be the population mass corresponding to the *case of flow convergence* shown in Figure 4(a), and let $m = m_2$ be the population mass for the example shown in Figure 4(b). Due to the fact that the current volume of the receptor reservoir v_r presented in the example of Figure 4(a) is greater than the current volume of the receptor reservoir presented in example Figure 4(b), then $m_1 < m_2$ since at the second scenario there is more available volume at the receptor reservoir. Similarly, comparing the examples shown in Figure 4(c), and 4(d) with population mass $m = m_3$, and $m = m_4$, respectively, it is obtained that $m_3 < m_4$ due to the available volume at the receptor reservoir.

Assumption 3: The n source reservoirs in the flow-convergence topology have the same discharge coefficients, i.e., $K_i = K$, for all $i \in \mathcal{S}$.   ◇

Assumption 3 implies a direct relationship between the constraint over the opening percentages in the valves and a constraint over the total inflow of the receptor reservoir. To clarify this fact, let $\tilde{v} = \max(v_1, \ldots, v_n)$ be the maximum current volume of the source reservoirs. Therefore, the maximum possible inflow to the receptor reservoir is constrained by the upper bound $Km\tilde{v}$. It follows that if the constraint $\sum_{i \in \mathcal{S}} K_i p_i = Km$ is considered, then according to Assumption 3, it is obtained that $\sum_{i \in \mathcal{S}} p_i = m$, which is a constraint over the opening percentages of the valves. As as result, the total inflow of the receptor reservoir is constrained by $\sum_{i \in \mathcal{S}} K p_i v_i \leq Km\tilde{v}$, where $m \in [0, 1]$ since $\ell = 1$.

According to the condition for the payoff functions in a UDS system presented in [77], the payoff function should be increasing with respect to the current volume at the source reservoir. Hence, the considered payoff function to control the *flow convergence* topology is selected considering the normalized outflows using the current volumes and the discharged coefficients, that is,

$$f_i(p_i) = - \underbrace{\left(\frac{1}{A\frac{v_i}{\bar{v}_i} + \varepsilon} \right)}_{\theta_i} p_i, \tag{22}$$

where A fixes the slope rate of the payoff function, and $\varepsilon \in \mathbb{R}_{>0}$ is a small factor that prevents an indetermination of f_i when the ith reservoir is empty. Moreover, the payoff function in (22) for the strategy $i \in \mathcal{S}$ only depends on the volume v_i and the proportion of agents p_i, making the

function appropriate in the decentralized control design due to the fact that only local information is required. Besides, the payoff function represents a full-potential game with potential function given by $V(\mathbf{p}) = -\frac{1}{2}\sum_{i \in \mathcal{S}}\theta_i p_i^2$, where $\theta_i > 0$, for all $i \in \mathcal{S}$. The potential function $V(\mathbf{p})$ is a strictly concave function. Therefore, according to Theorem 1, the existence of a strictly concave potential function implies the uniqueness of a Nash equilibrium.

Consider again the example shown in Figure 4(a), where $\frac{v_1}{\bar{v}_1} > \cdots > \frac{v_i}{\bar{v}_i} > \cdots > \frac{v_n}{\bar{v}_n}$, which implies that $\theta_1 > \cdots > \theta_i > \cdots > \theta_n$. Then, in the population game, it is expected that $p_1 > \cdots > p_i > \cdots > p_n$, assigning more priority to those reservoirs that are more filled up incrementing their outflow, and consequently avoiding overflows. More specifically, consider the example shown in Figure 4(a) with population mass $m = 1$, and with $n = 3$ whose discharge coefficients are equal, that is, $K_1 = K_2 = K_3 = 1$, and with parameters $A = 1$, and $\varepsilon = 0.1$. The maximum volumes of the reservoirs are $\bar{v}_1 = 15\,\mathrm{m}^3$, $\bar{v}_2 = 13\,\mathrm{m}^3$, and $\bar{v}_3 = 10\,\mathrm{m}^3$. Suppose that the current volumes at the reservoirs $1, 2$, and $3 \in \mathcal{S}$ are $v_1 = 10\,\mathrm{m}^3$, $v_2 = 5\,\mathrm{m}^3$, and $v_3 = 1\,\mathrm{m}^3$, respectively. Considering the payoff function of the form in (22), it is obtained $f_1 = -1.3043p_1$, $f_2 = -2.0635p_2$, and $f3 = -5p_3$. Therefore, the Nash equilibrium for this game is given by $p_1^* = 0.5283$, $p_2^* = 0.3339$, and $p_3^* = 0.1378$ since with this distribution it is obtained that $f_1(p_1^*) = f_2(p_2^*) = f_3(p_3^*)$. It follows that a bigger outflow is assigned to the fullest reservoir.

For the population dynamics design, the replicator dynamics with full information in (3) are implemented. Then, the closed-loop controller is completed for each stage within the whole UDS. The feedback is made by measuring information about the current volume at each reservoir, and by using the constant information about the maximum capacity at each reservoir. With this measured information, each controller finds the proper population mass and computes the proportion of agents in order to establish a proper control signal at the valves of each sub-system. The detailed closed-loop control scheme for each sub-system is presented in Figure 5.

It is worth noting that the way in which population dynamics are applied to solve engineering problems is flexible. This property is due to the fact that the key issue for designing population-dynamics-based controllers lies in the selection of the analogy between the engineering problem elements and the population game elements. This analogy is not unique in several cases. For instance, in the approach described in this section, the population mass was associated with the sum of the opening percentages of the source reservoirs valves. However, there exist other possible analogies, such as choosing the sum of the source reservoirs inflows as the population mass. In all cases, analogies have to be designed taking into account that population-dynamics-based controllers seek to dynamically distribute a certain resource among a set of entities to achieve a desired goal.

Case Study

The considered case study consists of the Bogotá (Colombia) stormwater UDS shown in Figure 6, which is divided into several *flow-convergence cases*. In this particular UDS, there are 163 sub-systems and, consequently, there are 163 decentralized population-games-based controllers. For instance, consider the segments of the UDS highlighted with blue color. These two parts of the network are presented in Figure 7. There are five different sub-systems in the segments presented in Figure 7 that are summarized in Table 2.

Figure 8 presents the communication layer, that is, it is shown 163 decentralized population-games-based controllers, the information that each controller measures and the control

actions that each controller establishes. Moreover, Figure 8 shows each closed-loop as the one presented in Figure 5.

The system is tested for an abrupt rain scenario that causes overflows. The direct run-off hydrographs that represent the system disturbances are presented in Figure 9.

Notice that the decentralized population-games-based controller is composed of N local controllers, then it is assumed that there is fully-available local information at each sub-system. The volumetric capacity of each reservoir is defined as the normalized volume of the ith reservoir denoted by $\tilde{v}$ that is, $\tilde{v} = v_i/\bar{v}_i$ where $\bar{v}_i$ is the maximum volume of the ith reservoir. Then, a flooding event occurs when the volume in a reservoir v_i is greater than $\bar{v}_i$, that is, when $\tilde{v} > 1$. Moreover, when considering normalized volumes, different reservoirs with different maximum capacities are compared properly according to an available capacity percentage. As previously said, the control objective is to avoid the overflows throughout the UDS. To this end, it is taken advantage of all the available volume capacities into the whole network. At each sub-system, there is a controller managing the outflows of the source reservoirs and distributing their current available capacity.

The evolution of the normalized reservoir volumes for the case without control are presented with blue color in Figure 10, whereas the evolution of the same reservoir volumes for the case with the decentralized population-games-based control are presented with black color in Figure 10. It can be seen that, with the decentralized population-games-based control, the overflows are avoided by doing an optimal distribution of flows throughout the system. Furthermore, the total volume of overflows for the case without control is $7770.2\,\mathrm{m}^3$, which is completely reduced with the designed decentralized population-game-based control, that is, the volume of wastewater released to the receptor environment is $0\,\mathrm{m}^3$ with the decentralized controller. It is pointed out that both cases with and without the population-games-based control are simulated with the same disturbances (rain events).

Concluding Remarks

Nowadays, engineering infrastructures are becoming complex systems given their large-scale nature complemented by the inherent nonlinearities of their compositional elements. Given that fact, several methods and approaches towards overcoming management and control problems for such large-scale systems have been presented and discussed, taking into account the concept of agents as baseline. Considering this modular methodology of splitting the system into subsystems related to agents, game theory, and particularly evolutionary game theory (EGT), appears as a way of handling the interaction between the agents defining the large-scale system in order to reach the control objectives seen as welfare relations within the EGT framework. This paper has highlighted the advantages of using EGT for the management and control of real engineering problems by means of showing the design and application of distributed control strategies for three relevant problems directly related to the framework of the smart cities. Specifically, this article shows the performance of EGT for designing local controllers towards fulfilling a global objective. This fact allows to implement non-centralized control strategies without a central coordinator and allowing to save computational time given the modularity of the entire control solution. Hence, this particular feature of a closed-loop topology based on EGT gives rise to considering other added advantages such as the potential inclusion of fault tolerance capabilities into the controller designs, key property when handling large-scale critical infrastructure systems.

In general, open problems related to the way the proposed control strategies must be decentralized, become scalable, and incorporate robust features may be discussed. In this sense, newer techniques should combine economic incentives, as well as the necessary amount of information to guarantee that we can add more elements to the system without having to entirely reconfigure the system. For the smart lighting application, the distributed characteristics of the proposed technique allow the algorithm to be implemented over large-scale systems with connected-graph communication structures. To solve resource allocation problems, the methodology facilitates the inclusion of new nodes to the network with simple plug-and-play controllers or special-purpose devices. In this sense, energy efficiency programs, demand response strategies, and optimization of wireless sensor networks can be considered as future work in the building automation field.

The distributed replicator dynamics approach used to solve the economic dispatch problem in the smart grid context could be extended to tackle several important issues such as including power losses, the physical power flow constraints, or the variability of renewable generation. Finally, regarding the UDS, although the proposed control approach can cope with overflows, more control objectives may be considered for their management, for instance, the minimization of operational costs given by the energy consumption of actuators to regulate the flows, or the minimization of the time spent for carrying the wastewater towards the treatment plant. The incorporation of additional control objectives are proposed as further work in the design of decentralized population-games-based controllers for UDS.

Acknowledgments

References

[1] G. Bacci, S. Lasaulce, W. Saad, and L. Sanguinetti, "Game theory for networks: A tutorial on game-theoretic tools for emerging signal processing applications," *IEEE Signal Processing Magazine*, vol. 33, pp. 94–119, Jan 2016.

[2] D. Vrabie, K. G. Vamvoudakis, and F. L. Lewis, *Optimal adaptive control and differential games by reinforcement learning principles*, vol. 81. IET, 2013.

[3] M. Zhu and E. Frazzoli, "Distributed robust adaptive equilibrium computation for generalized convex games," *Automatica*, vol. 63, pp. 82 – 91, 2016.

[4] L. Pavel, *Game theory for control of optical networks*. Springer Science & Business Media, 2012.

[5] W. Saad, Z. Han, H. V. Poor, and T. Basar, "Game-theoretic methods for the smart grid: An

overview of microgrid systems, demand-side management, and smart grid communications," *IEEE Signal Processing Magazine*, vol. 29, pp. 86–105, Sept 2012.

[6] Y. Wang, W. Saad, Z. Han, H. V. Poor, and T. Baar, "A game-theoretic approach to energy trading in the smart grid," *IEEE Transactions on Smart Grid*, vol. 5, no. 3, pp. 1439–1450, 2014.

[7] J. R. Marden and J. S. Shamma, "Game theory and distributed control," *Handbook of Game Theory*, vol. 4, pp. 861–899, 2014.

[8] S. Parsons and M. Wooldridge, "Game theory and decision theory in multi-agent systems," *Autonomous Agents and Multi-Agent Systems*, vol. 5, no. 3, pp. 243–254, 2002.

[9] J. Sanchez-Soriano, "An overview on game theory applications to engineering," *International Game Theory Review*, vol. 15, no. 03, p. 1340019, 2013.

[10] T. Basar and G. J. Olsder, *Dynamic noncooperative game theory*, vol. 23. Siam, 1999.

[11] I. Menache and A. Ozdaglar, *Network Games: Theory, Models, and Dynamics*. Morgan & Claypool Publishers, 2011.

[12] S. Lasaulce and H. Tembine, *Game theory and learning for wireless networks: fundamentals and applications*. Academic Press, 2011.

[13] W. H. Sandholm, *Population games and evolutionary dynamics*. Cambridge, Mass. MIT Press, 2010.

[14] R. A. Fisher, *The genetical theory of natural selection: a complete variorum edition*. Oxford University Press, 1930.

[15] J. Maynard Smith and G. Price, "The logic of animal conflict," *Nature*, vol. 246, p. 15, 1973.

[16] J. Maynard Smith, *Evolution and the Theory of Games*. Cambridge university press, 1982.

[17] M. A. Nowak and R. M. May, "Evolutionary games and spatial chaos," *Nature*, vol. 359, no. 6398, pp. 826–829, 1992.

[18] P. D. Taylor and L. B. Jonker, "Evolutionary stable strategies and game dynamics," *Mathematical biosciences*, vol. 40, no. 1, pp. 145–156, 1978.

[19] W. H. Sandholm, "Population games and deterministic evolutionary dynamics," *Handbook of game theory*, vol. 4, pp. 703–778, 2015.

[20] N. Li and J. R. Marden, "Designing games for distributed optimization," *IEEE Journal of Selected Topics in Signal Processing*, vol. 7, no. 2, pp. 230–242, 2013. Special issue on adaptation and learning over complex networks.

[21] J. R. Marden, S. D. Ruben, and L. Y. Pao, "A Model-Free Approach to Wind Farm Control Using Game Theoretic Methods," *IEEE Transactions on Control Systems Technology*, vol. 21, no. 4, pp. 1207–1214, 2013.

[22] H. Tembine, E. Altman, R. El-Azouzi, and Y. Hayel, "Evolutionary games in wireless networks," *IEEE Transactions on Systems, Man, and Cybernetics, Part B: Cybernetics*, vol. 40, no. 3, pp. 634–646, 2010.

[23] A. A. A. Abass, M. Hajimirsadeghi, N. B. Mandayam, and Z. Gajic, "Evolutionary game theoretic analysis of distributed denial of service attacks in a wireless network," in *2016 Annual Conference on Information Science and Systems (CISS)*, pp. 36–41, March 2016.

[24] I. Bomze, M. Pelillo, and V. Stix, "Approximating the maximum weight clique using replicator dynamics," *IEEE Transactions on Neural Networks*, vol. 11, no. 6, pp. 1228–1241, 2000.

[25] J. Poveda and N. Quijano, "Dynamic bandwidth allocation in wireless networks using a

shahshahani gradient based extremum seeking control," in *Proceedings of the 2012 6th International Conference on Network Games, Control and Optimization*, pp. 44–50, 2012.

[26] E. Mojica-Nava, C. Macana, and N. Quijano, "Dynamic population games for optimal dispatch on hierarchical microgrid control," *IEEE Transactions on Systems, Man, and Cybernetics: Systems*, vol. 44, pp. 306–317, March 2014.

[27] A. Pantoja and N. Quijano, "A population dynamics approach for the dispatch of distributed generators," *IEEE Transactions on Industrial Electronics.*, vol. 58, no. 10, pp. 4559 –4567, 2011.

[28] G. Obando, A. Pantoja, and N. Quijano, "Building Temperature Control based on Population Dynamics," *IEEE Transactions on Control Systems Technology*, vol. 22, no. 1, pp. 404–412, 2014.

[29] J. I. Poveda and N. Quijano, "Shahshahani gradient-like extremum seeking," *Automatica*, vol. 58, pp. 51–59, 2015.

[30] J. Barreiro-Gomez, N. Quijano, and C. Ocampo-Martinez, "Constrained distributed optimization: A population dynamics approach," *Automatica*, vol. 69, pp. 101–116, 2016.

[31] J. Barreiro-Gomez, G. Obando, G. Riaño Briceño, N. Quijano, and C. Ocampo-Martinez, "Decentralized control for urban drainage systems via population dynamics: Bogotá case study," in *Proceedings of European Control Conference*, pp. 2426–2431, 2015.

[32] L. García, J. Barreiro-Gomez, E. Escobar, D. Téllez, N. Quijano, and C. Ocampo-Martinez, "Modeling and real-time control of urban drainage systems: A review," *Advances in Water Resources*, vol. 85, pp. 120–132, 2015.

[33] J. R. Marden, "State based potential games," *Automatica*, vol. 48, no. 12, pp. 3075–3088, 2012.

[34] D. Fudenberg and J. Tirole, *Game Theory*. Cambridge, MA: MIT Press, 1991.

[35] G. Arslan and J. Shamma, "Distributed convergence to Nash equilibria with local utility measurements," in *Proceedings of the 43rd IEEE Conference on Decision and Control (CDC)*, vol. 2, pp. 1538–1543, 2004.

[36] N. Li and J. Marden, "Decoupling coupled constraints through utility design," *IEEE Transactions on Automatic Control*, vol. 59, no. 8, pp. 2289–2294, 2014.

[37] D. Palomar and M. Chiang, "A tutorial on decomposition methods for network utility maximization," *IEEE Journal on Selected Areas in Communications*, vol. 24, no. 8, pp. 1439–1451, 2006.

[38] P. A. Jensen and J. F. Bard, *Operations research models and methods*. John Wiley & Sons Incorporated, 2003.

[39] M. Batty, K. W. Axhausen, F. Giannotti, A. Pozdnoukhov, A. Bazzani, M. Wachowicz, G. Ouzounis, and Y. Portugali, "Smart cities of the future," *The European Physical Journal Special Topics*, vol. 214, no. 1, pp. 481–518, 2012.

[40] H. Chourabi, T. Nam, S. Walker, J. R. Gil-Garcia, S. Mellouli, K. Nahon, T. Pardo, and H. J. Scholl, "Understanding smart cities: An integrative framework," in *Proceedings of the 45th Hawaii International Conference on System Science*, pp. 2289–2297, 2012.

[41] B. Wollenberg and A. Wood, *Power generation, operation and control*. John Wiley & Sons, Inc, 1996.

[42] T. Ibaraki and N. Katoh, *Resource allocation problems: algorithmic approaches*. Cambridge, MA, USA: MIT Press, 1988.

[43] S. Ahn and S. Moon, "Economic scheduling of distributed generators in a microgrid

considering various constraints," in *Proceedings of the IEEE Power & Energy Society General Meeting.*, pp. 1–6, IEEE, 2009.

[44] J. Barreiro-Gomez, G. Obando, and N. Quijano, "Distributed population dynamics: Optimization and control applications," *IEEE Transactions on Systems, Man, and Cybernetics: Systems*, vol. 99, pp. 1–11, 2016.

[45] M. J. Smith, "The stability of a dynamic model of traffic assignment-an application of a method of lyapunov," *Transportation Science*, vol. 18, no. 3, pp. 245–252, 1984.

[46] L. E. Blume, "The statistical mechanics of strategic interaction," *Games and economic behavior*, vol. 5, no. 3, pp. 387–424, 1993.

[47] D. Ferraioli, "Logit dynamics: a model for bounded rationality," *ACM SIGecom Exchanges*, vol. 12, no. 1, pp. 34–37, 2013.

[48] R. Lahkar and W. H. Sandholm, "The projection dynamic and the geometry of population games," *Games and Economic Behavior*, vol. 64, no. 2, pp. 565–590, 2008.

[49] J. Weibull, *Evolutionary Game Theory*. The MIT press, 1995.

[50] A. Pantoja and N. Quijano, "Distributed optimization using population dynamics with a local replicator equation," in *Proceedings of the IEEE 51st Conference on Decision and Control (CDC)*, pp. 3790–3795, 2012.

[51] N. Gershenfeld, S. Samouhos, and B. Nordman, "Intelligent infrastructure for energy efficiency," *Science*, vol. 327, no. 5969, pp. 1086–1088, 2010.

[52] U.S. Energy Information Administration (EIA), "Annual energy outlook 2015," tech. rep., Department of Energy, 2015. Available on: www.eia.gov/forecasts/aeo/.

[53] International Energy Agency (IEA), *Guidebook on Energy Efficient Electric Lighting for Buildings*. Aalto University School of Science and Technology, 2015.

[54] A. Williams, B. Atkinson, K. Garbesi, E. Page, and F. Rubinstein, "Lighting controls in commercial buildings," *Leukos*, vol. 8, no. 3, pp. 161–180, 2012.

[55] A. Dounis and C. Caraiscos, "Advanced control systems engineering for energy and comfort management in a building environment: A review," *Renewable and Sustainable Energy Reviews*, vol. 13, no. 6-7, pp. 1246–1261, 2009.

[56] A. Dounis, P. Tiropanis, A. Argiriou, and A. Diamantis, "Intelligent control system for reconciliation of the energy savings with comfort in buildings using soft computing techniques," *Energy and Buildings*, vol. 43, no. 1, pp. 66–74, 2011.

[57] M. Koroglu and K. Passino, "Illumination balancing algorithm for smart lights," *IEEE Transactions on Control Systems Technology*, vol. 22, no. 2, pp. 557–567, 2014.

[58] Y. Wen and A. Agogino, "Control of wireless-networked lighting in open-plan offices," *Lighting Research and Technology*, vol. 43, no. 2, pp. 235–249, 2011.

[59] X. Cao, J. Chen, Y. Xiao, and Y. Sun, "Building-environment control with wireless sensor and actuator networks: Centralized versus distributed," *IEEE Transactions on Industrial Electronics*, vol. 57, no. 11, pp. 3596–3605, 2010.

[60] C. Ochoa, M. Aries, and J. Hensen, "State of the art in lighting simulation for building science: a literature review," *Journal of Building Performance Simulation*, vol. 5, no. 4, pp. 209–233, 2012.

[61] D. Forsyth and J. Ponce, *Computer Vision: A Modern Approach*. Prentice Hall Professional Technical Reference, 2002.

[62] V. Křivan, R. Cressman, and C. Schneider, "The ideal free distribution: a review and

synthesis of the game-theoretic perspective," *Theoretical Population Biology*, vol. 73, no. 3, pp. 403–425, 2008.

[63] R. Olfati-Saber, J. Fax, and R. Murray, "Consensus and cooperation in networked multi-agent systems," *Proceedings of the IEEE*, vol. 95, no. 1, pp. 215–233, 2007.

[64] J. Lopes, C. Moreira, and A. Madureira, "Defining control strategies for microgrids islanded operation," *IEEE Transactions on Power Systems*, vol. 21, no. 2, pp. 916–924, 2006.

[65] J. Hofbauer and K. Sigmund, *Evolutionary Games and Population Dynamics*. Cambridge UK: Cambridge University Press, 1998.

[66] N. Britton, *Essential mathematical biology*. NY Springer-Verlag, 2003.

[67] P. Young and S. Zamir, *Handbook of Game Theory with Economic Applications*, vol. 4. Elsevier, 2015.

[68] N. Quijano and K. Passino, "The ideal free distribution: Theory and engineering application," *IEEE Transactions on Systems, Man, and Cybernetics, Part B: Cybernetics.*, vol. 37, pp. 154 –165, feb. 2007.

[69] E. Mojica-Nava, C. Barreto, and N. Quijano, "Population games methods for distributed control of microgrids," *IEEE Transactions on Smart Grid*, vol. 6, no. 6, pp. 2586–2595, 2015.

[70] J. Giraldo and N. Quijano, "Delay independent evolutionary dynamics for resource allocation with asynchronous distributed sensors," in *Proceedings of the 3rd IFAC Workshop on Estimation and Control of Networked Systems*, vol. 3, pp. 121–126, 2012.

[71] A. Pantoja, N. Quijano, and K. M. Passino, "Dispatch of distributed generators under local-information constraints," in *Proceedings of the American Control Conference*, pp. 2682–2687, 2014.

[72] C. Ocampo-Martinez, *Model predictive control of wastewater systems*. Springer, 2010.

[73] V. Te Chow, *Open channel hydraulics*. McGraw-Hill Book Company, Inc; New York, 1959.

[74] R. Price and Z. Vojinović, *Hydroinformatics: Data, Models, and Decision Support for Integrated Urban Water Management*. Urban hydroinformatics series. IWA Publishing, 2011.

[75] V. Te Chow, *Open channel hydraulics*. McGraw-Hill Book Company, Inc; New York, 1959.

[76] E. Ramirez-Llanos and N. Quijano, "A population dynamics approach for the water distribution problem," *International Journal of Control*, vol. 83, no. 9, pp. 1947–1964, 2010.

[77] G. Riaño Briceño, J. Barreiro-Gomez, A. Ramirez-Jaime, N. Quijano, and C. Ocampo-Martinez, "MatSWMM - An open-source toolbox for designing real-time control of urban drainage systems," *Environmental Modelling and Software*, vol. 83, pp. 143–154, 2016.

Authors Information

Nicanor Quijano (IEEE Senior Member) received his B.S. degree in Electronics Engineering from Pontificia Universidad Javeriana (PUJ), Bogotá, Colombia, in 1999. He received the M.S. and PhD degrees in Electrical and Computer Engineering from The Ohio State University, in 2002 and 2006, respectively. In 2007 he joined the Electrical and Electronics Engineering Department, Universidad de los Andes (UAndes), Bogotá, Colombia as Assistant Professor. In 2008 he obtained the Distinguished Lecturer Award from the School of Engineering, UAndes. He is currently Full Professor and the director of the research group in control and automation systems (GIAP, UAndes). On the other hand, he has been a member of the Board of Governors of the IEEE Control Systems Society (CSS) for the 2014 period, and he was the Chair of the IEEE CSS, Colombia for the 2011-2013 period. Currently his research interests include: hierarchical and distributed optimization methods using bio-inspired and game-theoretical techniques for dynamic resource allocation problems, especially those in energy, water, and transportation. For more information and a complete list of publications see: https://profesores.uniandes.edu.co/nquijano/

Carlos Ocampo-Martinez (IEEE Senior Member) received his Electronics Engineering degree and his MSc. degree in Industrial Automation from Universidad Nacional de Colombia, Campus Manizales, in 2001 and 2003, respectively. In 2007, he received his Ph.D. degree in Control Engineering from the Technical University of Catalonia (Barcelona, Spain). Since 2011, he is with the Technical University of Catalonia, Automatic Control Department (ESAII) as Associate Professor in automatic control and model predictive control. Since 2014, he is also Deputy Director of the Institut de Robòtica i Informàtica Industrial (CSIC-UPC), a Joint Research Center of UPC and CSIC. His main research interests include constrained model predictive control, large-scale systems management (partitioning and non-centralized control), and industrial applications (mainly related to the key scopes of water and energy). For more information, see: http://www.iri.upc.edu/people/cocampo/

Julian Barreiro-Gomez received his B.S. degree in Electronics Engineering from Universidad Santo Tomas (USTA), Bogotá, Colombia, in 2011. He received the MSc. degree in Electrical Engineering from Universidad de Los Andes (UAndes), Bogotá, Colombia, in 2013. Since 2012, he is with the research group in control and automation systems (GIAP, UAndes), where he is pursuing the Ph.D. degree in Engineering in the area of control systems. Since 2014, he is associate researcher at Technical University of Catalonia (Barcelona, Spain), Automatic Control Department (ESAII), and Institut de Robòtica i Informàtica Industrial (CSIC-UPC), where he is pursuing the Ph.D. degree in Automatic, Robotics and Computer Vision. His main research interests are constrained model predictive control, distributed optimization and control, game theory, and population dynamics.

Germán Obando received the B.S. degree in Electronics Engineering from Universidad de Nariño, Pasto, Colombia, in 2008. He received the M.S. and the PhD. degree in Electronics Engineering from Universidad de los Andes, Bogotá, Colombia, in 2010 and 2016, respectively. Currently, he is a postdoctoral fellow in the research group in control and automation systems (GIAP, Universidad de los Andes), and part of the ALTERNAR project. His main research interests are distributed optimization, population dynamics, and game theory.

Andrés Pantoja received the B.S. degree in Electronics Engineering from Universidad Nacional, Manizales, Colombia, in 1999, the M.S. degree, and the PhD. degree in Electronics Engineering from Universidad de los Andes, Bogotá, Colombia, in 2008 and 2012, respectively. In 2003, he joined Departamento de Electrónica, Universidad de Nariño, Pasto, Colombia, where he is currently Assistant Professor, director of the research group on electrical and electronics engineering (GIIEE), and head of the ALTERNAR project. The research interests are dynamic resource allocation, distributed generation, distributed control in smart grids and buildings, and coordination in large-scale systems.

Eduardo Mojica-Nava received the B.S. degree in electronics engineering from the Universidad Industrial de Santander, Bucaramanga, Colombia, in 2002, the M.Sc. degree in electronics engineering from the Universidad de Los Andes, Bogotá, Colombia, and the Ph.D. degree in automatique et informatique industrielle from the Ecole des de Nantes, Nantes, France in co-tutelle with Universidad de Los Andes, in 2010. He is currently an Associate Professor with the Department of Electrical and Electronics Engineering, National University of Colombia, Bogotá, Colombia. His current research interests include optimization and control of complex networked systems, switched and hybrid systems, and control in smart grids applications.

Sidebar: *Rock-paper-scissors* game in a population with different types of interactions

The strategies employed by the individuals within a population can constraint their interactions. To illustrate this fact, consider the example depicted in Figure S1. This figure shows two populations where individuals are playing the classic *rock-paper-scissors* game. Assuming that players can only be matched with their neighbors, each population exhibits a different type of interactions. On the one hand, Figure S1(a) shows a population with unconstrained interactions since a player that chooses a certain strategy can interact with players that choose any other strategy. For instance, consider the payer marked with the circle drawn in solid blue line. The neighborhood of this player (which is marked with the circle drawn in dashed red line) contains individuals playing all the available strategies. On the other hand, Figure S1(b) shows the same population game, but with strategy-constrained interactions. In this case, notice that the allowed interactions depend on the strategies of players. For instance, an individual that choose *scissors* to play can not encounter an individual playing *rock*.
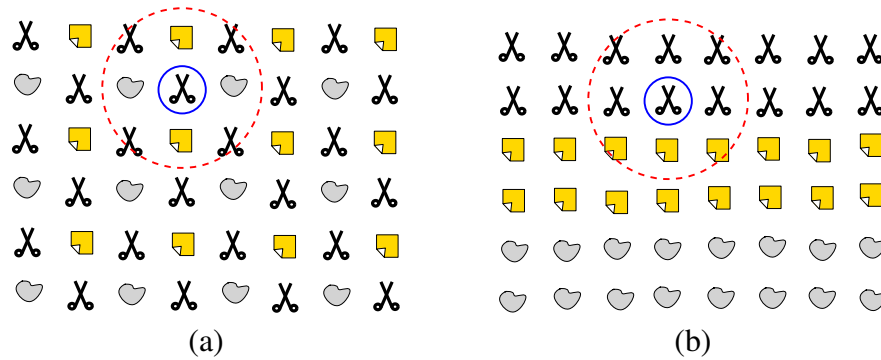
Figure S1.   A population game with two different types of interactions: (a) Unconstrained interactions. (b) Strategy-constrained interactions. Each element represents a player, and the shape of the element (*rock*, *paper*, or *scissors*) denotes the strategy that the player has adopted. Notice that, in populations with unconstrained interactions, each player can interact with individuals that are playing any strategy. By contrast, in populations with constrained interactions, allowed interactions are restricted by players' strategies.

Sidebar: The relationship among matricial games, full-potential population games, and resource allocation problems

Matrix game

Consider a two-player symmetric matricial game as in Table S1.

TABLE S1

MATRICIAL REPRESENTATION OF THE COORDINATION GAME

		Player 2		
		1	**2**	**3**
Player 1	**1**	-1,-1	0,0	0,0
	2	0,0	-2,-2	0,0
	3	0,0	0,0	-3,-3

This game is known as coordination game. Assigning a different interpretation of the game, suppose that each player represents an animal selecting among three possible habitats from the set of strategies $\mathcal{S} = \{1, 2, 3\}$, which represent the strategies. The payoff describes the amount of available food and/or the reproduction chances. Players one and two select a strategy in order to maximize their utilities denoted by u_1, and u_2, respectively.

Moreover, suppose that player one selects strategies $1, 2$, and $3 \in \mathcal{S}$ with probabilities $\mathbf{p}^1 = [p_1^1 \quad p_2^1 \quad p_3^1]^\top$, whereas player two selects the same strategies with probabilities $\mathbf{p}^2 = [p_1^2 \quad p_2^2 \quad p_3^2]^\top$, where $\sum_{i=1}^{3} p_i^1 = 1$, and $\sum_{i=1}^{3} p_i^2 = 1$. The Nash equilibrium is given by $\mathbf{p}^{1*} = \mathbf{p}^{2*} = [6/11 \quad 3/11 \quad 2/11]$, since under this scenario, there is no incentive for any player to change their strategic distribution to increase their utilities. Let $\mathbb{E}_1(\mathbf{p}^1, \mathbf{p}^2)$ be the expected utility of player one given by

$$\mathbb{E}_1 = -p_1^1 p_1^2 - 2 p_2^1 p_2^2 - 3(1 - p_1^1 - p_2^1)p_3^2,$$
$$= -0.54,$$

and, let $\mathbb{E}_2(\mathbf{p}^1, \mathbf{p}^2)$ be the expected utility of player one given by $\mathbb{E}_2 = -0.54$.

Population game

Now, consider a population composed of a large and finite number of animals which may select among three different habitats given by $\mathcal{S} = \{1, 2, 3\}$. Figure S2 shows the population and each color corresponds to a strategy. Animals can interact each other to compare their utilities and determine whether it is better to change habitat.

The scalar $p_i \in \mathbb{R}_{\geq 0}$ represents the proportion of animals selection the strategy $i \in \mathcal{S}$. Moreover, $\mathbf{p} \in \mathbb{R}^n$ is the population state, and the set of possible population states is given by
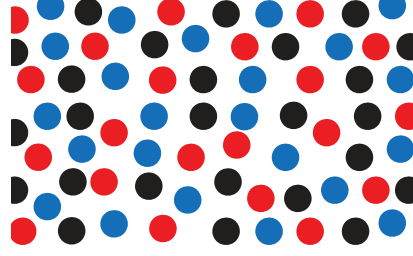
Figure S2. A population with three available colored strategies.

$\Delta = \{\mathbf{p} \in \mathbb{R}^n_{\geq 0} : \sum_{i \in \mathcal{S}} p_i = 1\}$. Payoff functions are given by

$$\mathbf{f}(\mathbf{p}) = \begin{bmatrix} -1 & 0 & 0 \\ 0 & -2 & 0 \\ 0 & 0 & -3 \end{bmatrix} \mathbf{p}.$$

The evolution of the population states $\mathbf{p}$ for three different initial conditions under the replicator dynamics are shown in Figure S3. Notice that all the trajectories converges to the equilibrium
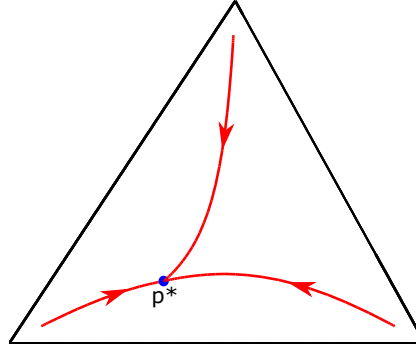

Figure S3. Evolution of proportion of animals to the equilibrium point from three different initial conditions.

point $\mathbf{p}^* = [6/11 \quad 3/11 \quad 2/11]$.

Potential games and resource allocation problems

The coordination game is a full-potential game with potential function

$$V(\mathbf{p}) = -\frac{1}{2}p_1^2 - p_2^2 - \frac{3}{2}p_3^2,$$

since $\mathbf{f}(\mathbf{p}) = \nabla V(\mathbf{p})$. The potential function and its projection over the simplex are presented in Figure S4. Notice that the Nash equilibrium coincides with the maximum point in the potential function. Consequently, it is possible to maximize a function subject to the constraint given by the simplex
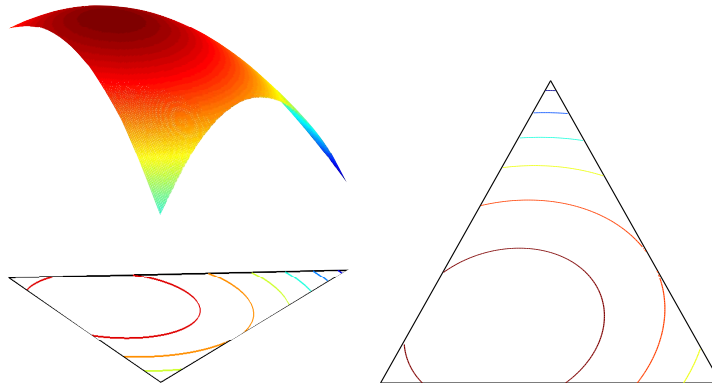
Figure S4. Potential function and its contour projection over the simplex.

$$\max_{\mathbf{p} \in \Delta} V(\mathbf{p}),$$

subject to

$$\sum_{i \in S} p_i = 1,$$

$$p_i \geq 0, \text{ for all } i \in \mathcal{S}.$$

The optimization problem is of the same form as a resource allocation problem with a concave cost function and constraints related to a total resource and positivity.

Sidebar: An experimental testbed for lighting systems

A lighting environment is represented by the testbed shown in Figure S5, where luminaries are small incandescent lamps in the roof of the box and sensors are the photocells in the floor. The lamps are driven by power amplifiers and the sensor signals are obtained by a voltage-divider array interfaced by a dSPACE DS1104 DAQ board to Simulink programs.

Figure S5. Experimental testbed to model an eight-zones environment. Each zone composed by close lamps and photocells can be divided by "walls" to emulate different cross-illumination conditions. The control strategy is implemented in Simulink through a dSPACE DS1104 DAQ board.

The environment is divided in eight zones, each one with a lamp and a sensor distributed unevenly across the room. In this representation, the influence among zones or cross-illumination can be varied by cardboard "walls" or partitions with different heights, such that the higher the divisions, the lower the influence of other zones. Therefore, open or divided environments can be emulated. Moreover, the box has a window in the rightmost side to simulate daylight and show the effects of this disturbance over the system. The control goal is to reach a desired illuminance setpoint at each zone with a limited available power, handling disturbances and inter-zone effects.
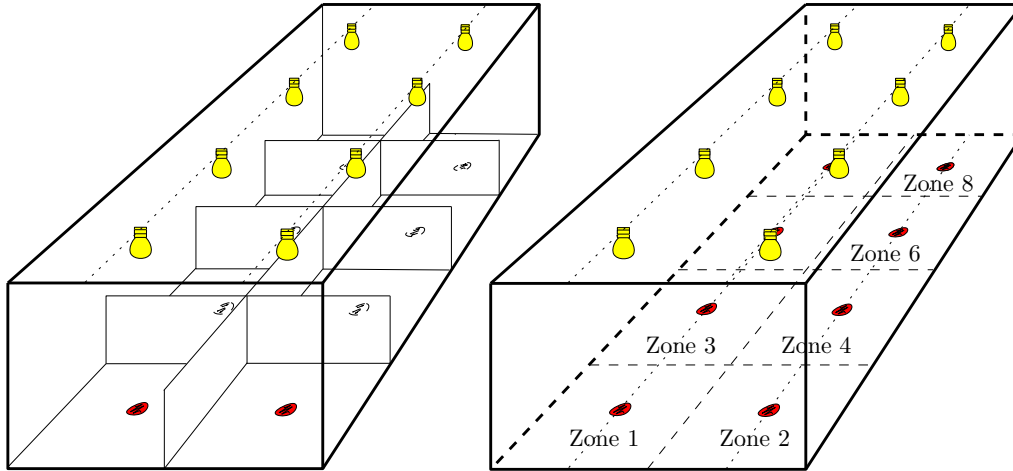
Figure S6. Testbed schematics of different environments. The former (left) emulates a system with cubicles separated by half-size walls. The latter (right) represents an open environment with high cross-illuminance effects. The resource allocation process is performed to split a selected available voltage among the lamps to obtain desired illuminations in each zone. Therefore, the second case is more challenging because of the significant variable coupling.

Two cases are considered to show the adaptability of the population-based methodology. The first case represents a lighting system with half-size divisions, such that the cross-illumination is not negligible, but reduced. The second case is an open environment to observe the effect of coupling among zones and how to use it to provide energy savings. A schematic of the two environments is presented in Figure S6. In both cases, it is assumed that the resources are enough to achieve the desired illumination levels in the environments.

Sidebar: Muskingum model

The Muskingum model is a linear hydrological-based model that allows to describe the behavior of UDS by using the mass conservation principle. For the ith reservoir is given by the following differential equation and relation between its inflows and outflows [S1]

$$v_i = \gamma_i \left(I_i l_i + O_i(1 - l_i) \right),$$
$$\dot{v}_i = I_i - O_i,$$

where v_i is the volume of the reservoir, γ_i is a parameter for the model calibration, l_i is the reservoir length, and I_i and O_i are the inflows and outflows, respectively. Then, by expressing the outflows as function of v_i, I_i, l_i, and γ_i, it is obtained that

$$\dot{v}_i = \frac{1}{1 - l_i} \left(I_i - \frac{v_i}{\gamma_i} \right)$$
$$\dot{v}_i = q_{in,i} - K_i p_i v_i,$$

where $q_{in,i} = I_i/(1 - l_i)$, $q_{out,i} = K_i p_i v_i$, and $K_i p_i = 1/(\gamma_i - \gamma_i l_i)$. Furthermore, $p_i \in [0, 1]$ determines the control input over the output gate, which sets its grade of opening (that is, zero is completely closed, and one is completely opened).

References

[S1] V. Te Chow, *Open channel hydraulics*. McGraw-Hill Book Company, Inc; New York, 1959.

List of Figures
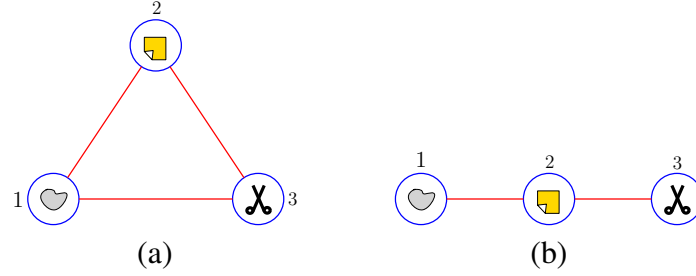
Figure 1. Graph representation of the two types of interactions described in Figure S1: (a) Unconstrained interactions. (b) Strategy-constrained interactions. For notational purpose the available strategies are indexed (1 corresponds to *rock*, 2 corresponds to *paper*, and 3 corresponds to *scissors*). Notice that, while unconstrained interactions are represented by complete graphs, strategy-constrained interactions are represented by non-complete graphs
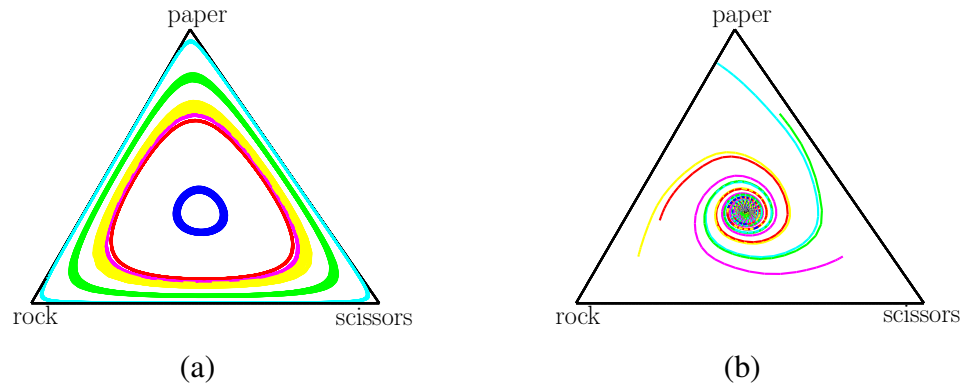

Figure 2. Trajectories of the *rock-paper-scissors* game under two population dynamics: (a) Replicator dynamics. (b) Smith dynamics. Each color corresponds to a trajectory generated with a different initial condition. Notice that all the trajectories are inside the simplex Δ, whose limits are drawn in black color. This fact is given since replicator and Smith dynamics satisfy mass conservation and nonnegativity of the states.
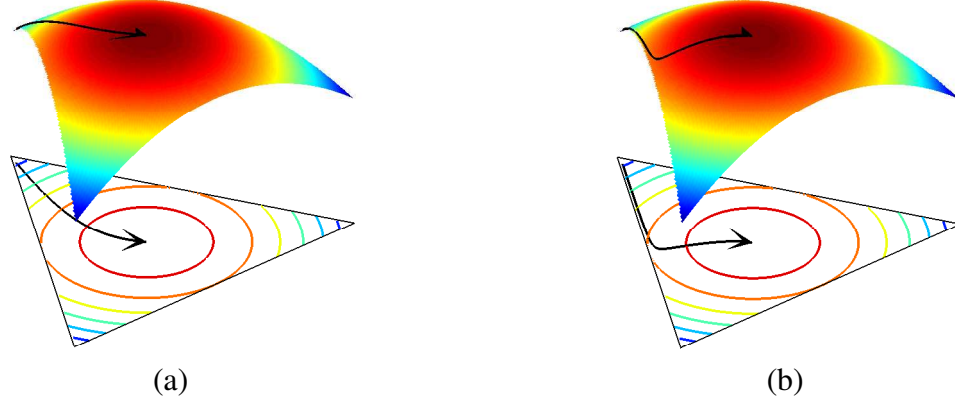
Figure 3. Convergence to Nash equilibrium in a full-potential game under: (a) Replicator dynamics. (b) Distributed replicator dynamics. A population playing a full-potential game and evolving following these dynamics tends towards the Nash equilibrium of the game. In addition, the Nash equilibrium matches the maximizer of the potential function.
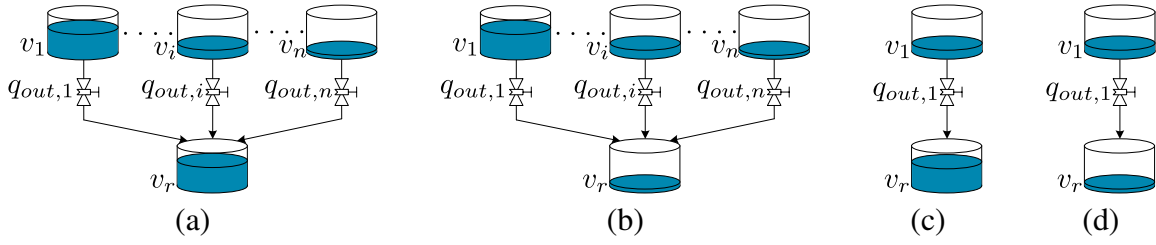

Figure 4. (a) and (b) exhibit a convergence topology with n source reservoirs and one receptor reservoir [31]. (c) and (d) exhibit a particular case of convergence topology with only one source reservoir.
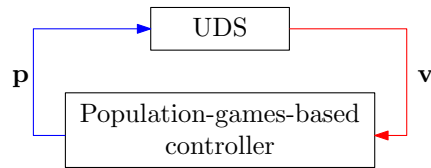
Figure 5. Closed loop for each sub-system (partition) of the UDS.
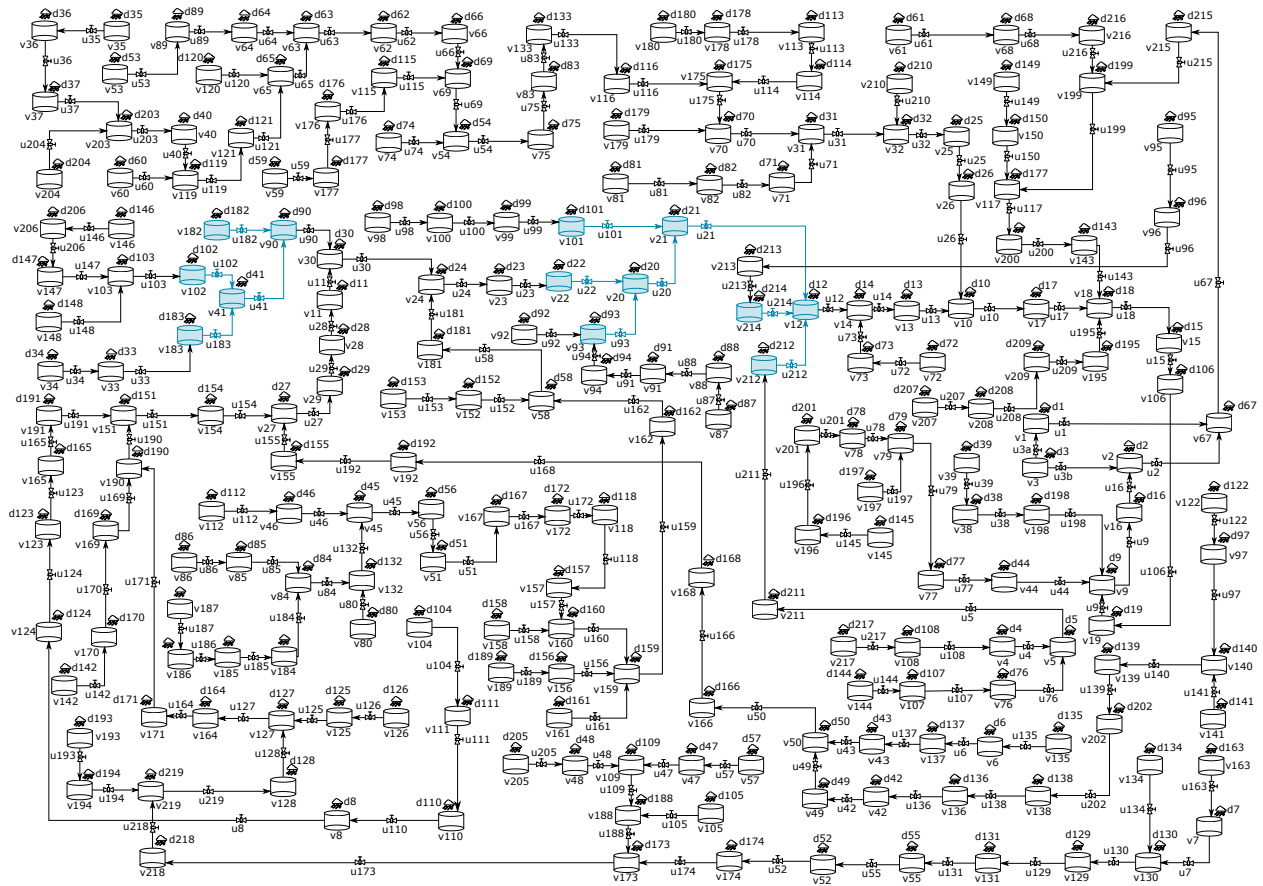
Figure 6.   Large-scale drainage system in Bogotá-Colombia. The network at the Chicó neighborhood, which is located at the north of the city. This UDS system has 219 sub-catchments that drain to 219 collection chambers. Clusters of different catchments are simplified into reservoirs as in [72], and the system dynamics for control purposes are modeled with the Muskingum linear reservoir model.
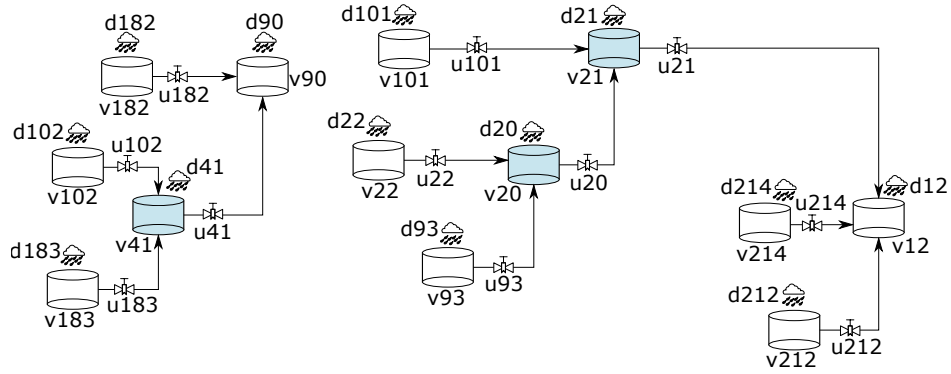
Figure 7. Example of five sub-systems, each one of them with various source reservoirs and only one receptor reservoir. Some reservoirs (for example those highlighted into the figure) might be source and receptor for two different partitions, simultaneously. The sub-systems are composed of reservoirs 41, 102, and 183; 41, 90, and 182; 20, 22, and 93; 20, 21, and 101; 12, 21, 212, and 214.

Figure 8. Communication layer for each controller. The red arrows correspond to the measured information, and the blue arrows correspond to the computed control inputs. Each controller presented by gray circles has a closed-loop scheme as the one presented in Figure 5. Furthermore, notice that the controllers are local and use partial information from the UDS. Besides, due to the fact each controller only computes a small portion of the total control inputs, the computational burden is reduced with respect to a centralized controller computing the 219 control inputs.

Figure 9. 219 Direct run-off hydrograph. The run-off hydrograph $d_i = 0$ for $i = \{1, ..., 219\}$ in the interval of time $0[\text{hours}] \leq t \leq 40[\text{hours}]$, and $70[\text{hours}] \leq t \leq 480[\text{hours}]$. These rain events are unknown and considered as disturbances for the UDS.
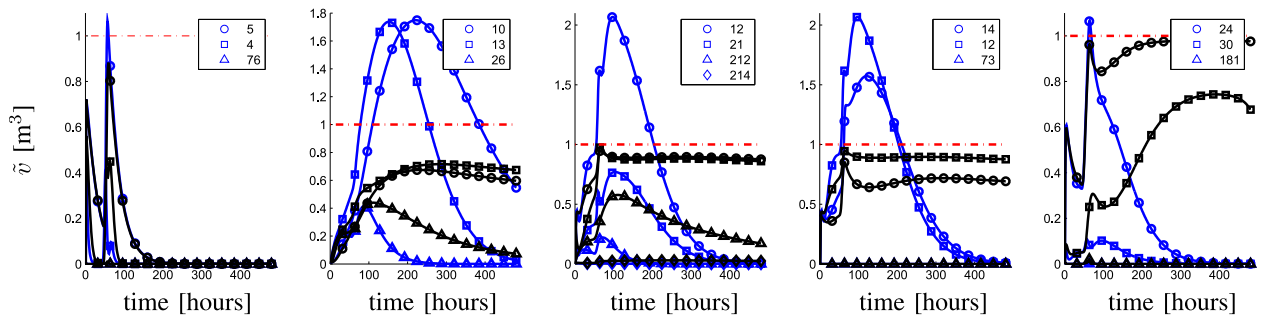

Figure 10. Evolution of normalized volumes along 20 days. Blue lines correspond to the scenario without control, and black lines correspond to the scenario with decentralized population-games-based control. Figure shows the evolution of the normalized reservoirs volume where overflows occur without control, that is, reservoirs $5, 10, 12, 13, 14$, and 24; and their involved reservoirs in the same local controller, that is, $4, 21, 26, 30, 73, 76, 181, 212$, and 214 (these reservoirs correspond to the controllers $c_{123}, c_{53}, c_{63}, c_{49}$, and c_{59}).
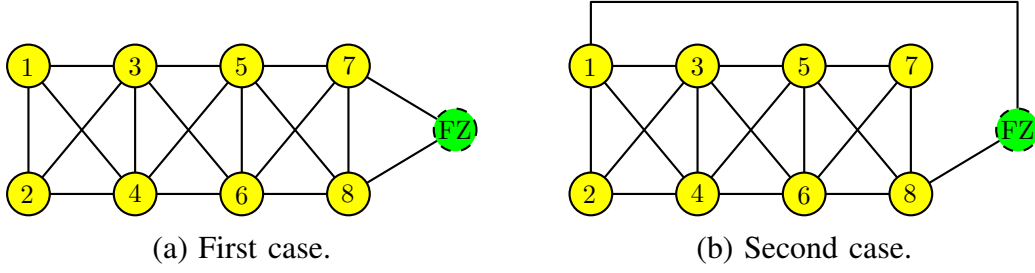
(a) First case. (b) Second case.

Figure 11. Graph structures for the lighting system. Given the network structure for the real zones, the inclusion of the fictitious zone (FZ) requires an extra link between nodes 1 and 8 only in the second case, since in the first one, there already exists the link $(7, 8)$.
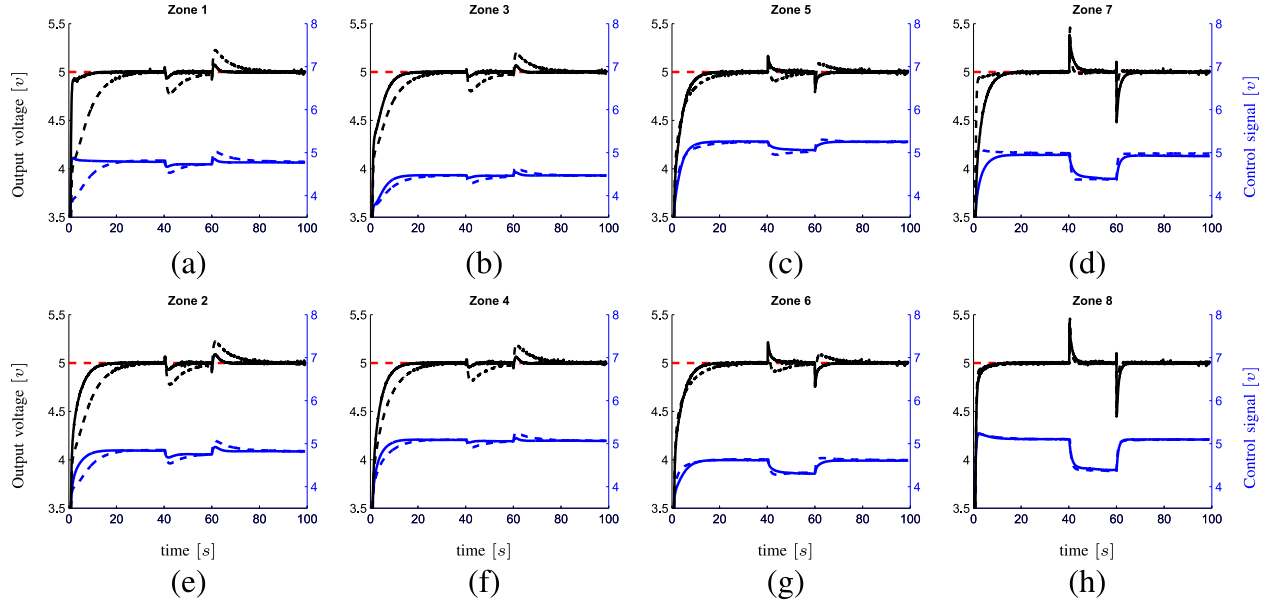

Figure 12. Testbed results for the divided environment. Dashed and solid lines represent the responses for the networks in cases 1 and 2, respectively. Illuminance of each zone (left axis and black lines) and voltage applied to each lamp (right axis and blue lines) are shown for the two cases, while the illuminance set point (E_{set}) is presented in red. The desired uniform illuminance is reached in all zones even when a disturbance is applied between $t = 40$ s and $t = 60$ s. The disturbance emulates daylighting through a window in the environment.
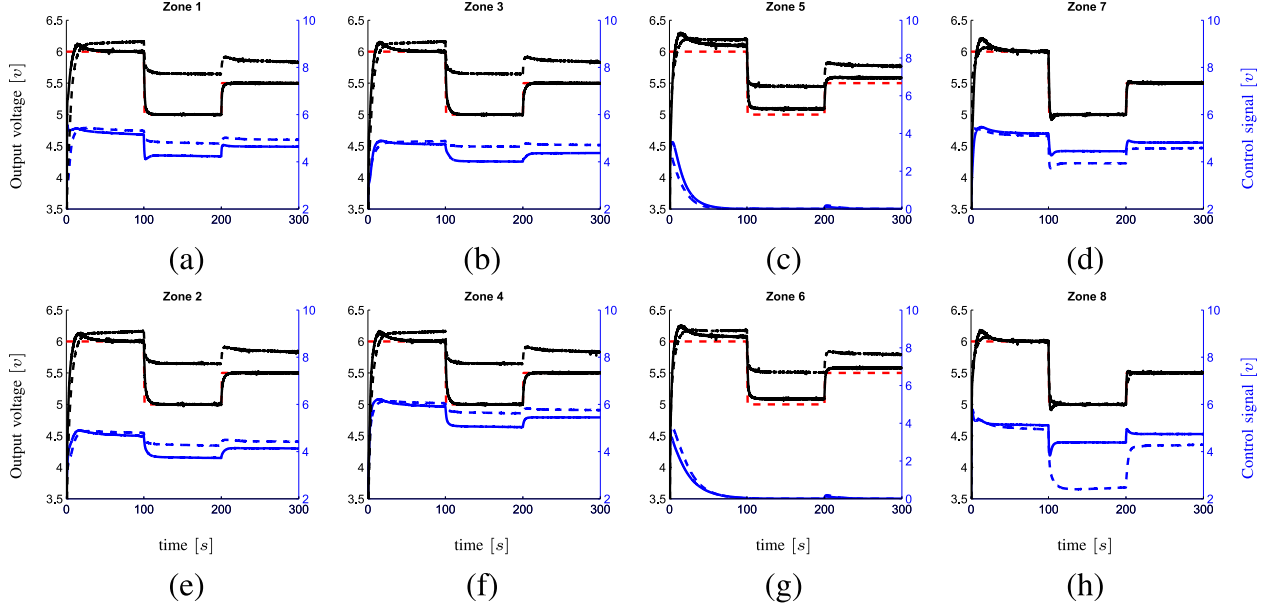
Figure 13. Testbed results for the open environment. Dashed and solid lines represent the responses for the topologies in cases 1 and 2, respectively. Illuminance of each zone (left axis and black lines) and voltage applied to each lamp (right axis and blue lines) are shown for the two cases, while the changes in illuminance setpoints (E_{set}) are presented by the red line. Due to the truncation of zones 5 and 6, the resource allocation within the first network is not successful due to the formation of unconnected components. In the second case, the fictitious zone connects the graph and the desired setpoints are reached except in the truncated zones.
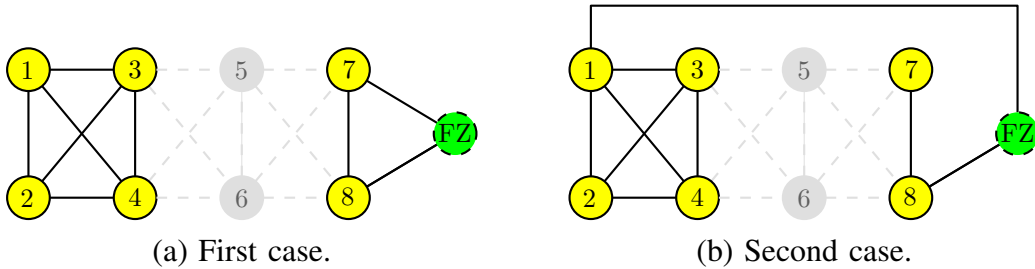

Figure 14. Graph structures with truncated zones. In the first case the truncation splits the graph into two components. The location of the fictitious zone (FZ) in the second case connects the graph despite of the truncated zones.
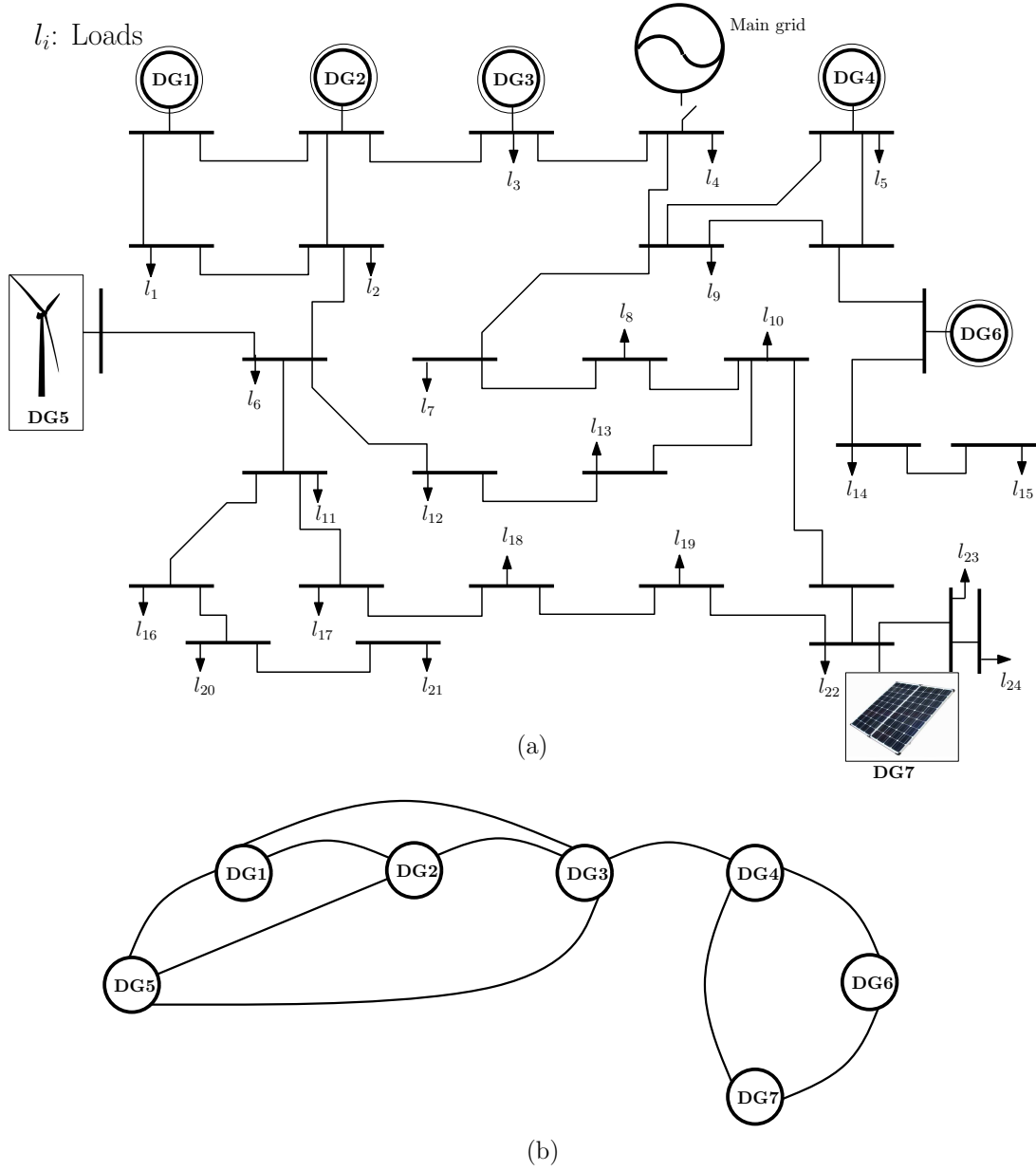
l_i: Loads

(a)

(b)

Figure 15. Microgrid test system with seven distributed generators and several loads: (a) An illustrative general scheme of a microgrid model adopted from a IEEE 30-bus distribution system and (b) graph representing the topology of the communication network between DGs.
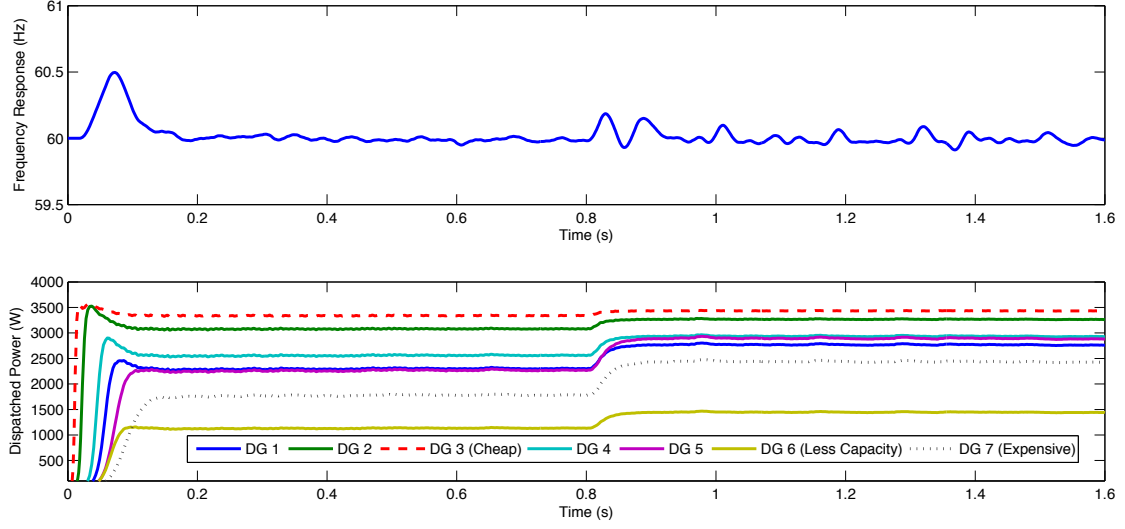
Figure 16. Results obtained with distributed replicator dynamics for the microgrid test system: (a) frequency response at the main grid bus, and (b) DGs active power response. As seen in (a), the distributed replicator dynamics returns the operating frequency of the mcirogrid to its nominal value. Figure (b) shows that when the demand is increased at $t = 0.8$ s, the expensive generator DG 7 increases its power to compensate the demand constraint.

List of Tables

TABLE 1
EQUIVALENCE RELATIONSHIPS BETWEEN POPULATION DYNAMICS AND APPLICATION CASES

Population dynamics	UDS	Lighting Systems	Microgrids
Population	System	Lighting environment	Power dispatch
Strategy	Source reservoirs	Lighting zones	Distributed generators
Population mass	Total inflow to receptor reservoir	Total available voltage	Total demanded power
Agent	Flow unit	Voltage unit	Power unit
Proportion of agents	Proportion of flow	Proportion of voltage	Proportion of power
Strategic distribution	Flow distribution in source reservoirs	Voltage split among lamps	Economic power dispatch
Payoff of a strategy	Current volume	Tracking error	Marginal utility

TABLE 2
DESCRIPTION OF THE SUB-SYSTEMS PRESENTED IN FIGURE 7.

Source reservoirs	Receptor reservoir
$102, 183$	41
$41, 182$	90
$22, 93$	20
$20, 101$	21
$21, 214, 212$	12